行政院國家科學委員會專題研究計畫　成果報告

GMPLS 網路架構下的網路流量控衡(2/2)

計畫類別： 個別型計畫
計畫編號： NSC93-2213-E-009-027-
執行期間： 93 年 08 月 01 日至 94 年 07 月 31 日
執行單位： 國立交通大學資訊科學學系(所)

計畫主持人： 陳健

報告類型： 完整報告
報告附件： 出席國際會議研究心得報告及發表論文
處理方式： 本計畫可公開查詢

中　華　民　國 94 年 10 月 27 日

ABSTRACT

The objective of the project is to study the traffic engineering issues in the GMPLS (Generalized Multi-Protocol Label Switching) network and develop promising algorithms to maximize the network resource utilization and throughput while minimizing both the end-to-end delay and network instability. GMPLS is extension of MPLS (Multi-Protocol Label Switching). With some modification and additions to the MPLS routing and signaling protocol, the GMPLS can be used not merely with router, but also with newer device like OXC (Optical Cross-Connect). The wavelengths in OXC can be treated as labels. These modifications are being standardized by the Internet Engineering Task Force (IETF). However, there are remaining challenges to adapt a traffic engineering scheme, which optimize network utilization, under a dynamic change of real IP traffic in GMPLS network, such as logical topology design problem, routing and wavelength assignment (RWA) problem, protection/restoration problem, etc.

In this report, we present several heuristic algorithms to solve the problems stated above in the networks that utilize multi-granularity optical cross-connects (MG-OXCs) as their node architecture. Simulation results are also shown respectively to validate our algorithms.

Keywords: DWDM, Generalized Multi-Protocol Label Switching (GMPLS), traffic engineering, hierarchical cross-connect

中文摘要

本計畫的目的在於學習 GMPLS（Generalized Multi-Protocol Label Switching）網路的傳出工程以及發展出適合的演算法來增進網路資源的利用率與流量，以及將網路傳輸的延遲及不穩定性降到最低。GMPLS 為 MPLS（Multi-Protocol Label Switching）的延伸，原本 MPLS 上的路由協定與信號協定經過一些修改與增加之後，GMPLS 不僅能適用在路由器上，而且也能適用在像 OXC（Optical Cross-Connect）等較新的設備上，因為波長在 OXC 上就被視同為原本 MPLS 上的標籤。目前 IETF 正在進行 GMPLS 相關協定的修改與標準化。然而，動態的 IP 流量在 GMPLS 網路之下，仍然存在著一些網路傳輸工程的挑戰需要被克服，例如邏輯拓僕設計問題、路徑與波長分配問題、網路保護與修復問題等等。

在本報告中，我們總結了我們所提出的數個解決在多單位光交換器網路中所會遭遇的上述問題的啟發式演算法。報告也將個別展示我們的模擬結果來證實我們所提出的演算法的可行性。

關鍵詞: DWDM，GMPLS，流量控衡，多單位光交換器

TABLE OF CONTENT

Chapter 1. Introduction

With the advance of electrical and optical technologies, high-performance IP routers and high-capacity OXC systems have been widely deployed in today's core network. The routers perform packet forwarding, traffic aggregation, and demultiplexing and thus achieve high link utilization. The OXCs set up optical label switching paths (OLSPs, i.e., lightpaths) between the IP routers based on the IP traffic between the routers. Because of fluctuation of IP traffic, it is necessary to measure IP traffic and monitor network congestion status to dynamically configure the OLSPs so as to maximize network resource utilization. This is so-called traffic engineering. GMPLS (Generalized Multi-Protocol Label Switching) [Berger01] signaling/routing protocols provide the necessary linkage between the IP and photonic layers, allowing interoperable, scalable, parallel, and cohesive evolution of networks in the IP and photonic dimensions. Therefore, we proposed using GMPLS to perform traffic engineering on future telecom network.

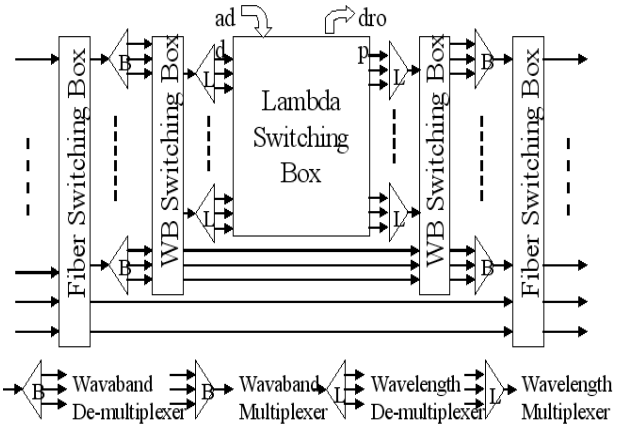

The MG-OXC architecture.

We consider hierarchical wavelength-division-multiplexed (WDM) networks with different switching granularity. Multi-granularity Optical Cross Connect (MG-OXC), shown in the figure above, is used to bundle wavelengths into a waveband or a fiber tunnel. It is attractive for its scalability and cost reason. However, the solutions to satisfy lightpath requests, to some extent, become different to that of the conventional WDM networks.

In this report, we focus on the following issues on the MG-OXC networks

1. Routing and wavelength assignment (RWA)
2. Protection
3. Virtual topology reconfiguration

This report is organized as follows. Chapter 2 introduces a graph model for characterizing the MG-OXC networks and proposes an effective heuristic for RWA in MG-OXC networks. In chapter 3,

RWA in MG-OXC networks is formalized as an integer linear programming (ILP) problem. Chapter 4 presents the heuristics for protection problem in MG-OXC networks while chapter 5 is for restoration problem. We conclude in chapter 6.

Chapter 2. An Effect Scheme for Fixed-length Tunnel Allocation in Hierarchical WDM Networks

I. Introduction

Wavelength-division-multiplexing (WDM) networks have emerged as a method of providing Terabits-per-second capacity for ever-increasing bandwidth demands. While increase in number of wavelength channels and fibers between node pairs may increase available capacity, the resultant managing complexity and switching fabric of optical cross-connects (OXCs) also increase. An effective way of handling this problem is to bundle a group of consecutive wavelength channels together and switch them as a single unit on the specific route to reduce the required resources of intermediate cross-connects along the route. The tunnel-like passage created by the bundled wavelength channels is defined as a waveband/fiber tunnel. Wavelengths in a tunnel must be switched together except at the two ends of the tunnel. Nodes that support such multigranularity switching, e.g. wavelength, waveband and fiber-switching, is termed hierarchical cross-connects or multigranularity optical cross-connects (MG-OXCs).

Generally, the research topics about MG-OXCs can be categorized into (a) given the network resources, minimize the blocking probability of the coming requests, and (b) dimension the network resources when given the set of traffic requests. In [HaSh01], merits of hierarchical OXC, or MG-OXC, were summarized such as small-scale modularity, reduced cross-talk, and the reduced of complexity. [NoVi01] showed that the number of ports required when grouping of consecutive lightpaths are applied to the network (excluding grouping the traffic from different source nodes to different destination nodes) can be significantly reduced. In [HoMa01] a novel switching architecture, MG-OXC was proposed to minimize the blocking probability for the dynamic requests given the limited network resources. In [LeYu01], which employs a two-stage scheme of waveband and wavelength, an integer linear programming (ILP) formulation and a heuristic are given that aim to group lightpaths with the same destination only, while in [CaAn01] both the ILP and heuristic were given to handle the more general cases. Continuing with [CaAn01], [CaAn02] further studies Single-Layer MG-OXCs and Multi-Layer MG-OXCs under both off-line and on-line traffic.

In this chapter, we consider the following network design problem. Given fixed amount of network resources and a historical traffic matrix that the dynamic requests will follow, the objective is to determine a set of tunnels that minimize the blocking probability for the dynamic traffic requests. The heuristic Capacity-Balanced Static Tunnel Allocation (CB-STA) [HoMa01] has been proposed that first estimates the amount of traffic traveling through each node by routing the historical traffic matrix in the network. Then the nodes with maximal traffic going out and maximal

traffic coming in are selected repeatedly for tunnel allocation. To efficiently utilize the wavelength ports and fibers, each node pair selected for tunnel allocation is required to follow a tunnel length constraint, i.e., each tunnel should be equal to an average hop distance. However, CB-STA does not consider the tunnel length constraint when picking the node pairs, resulting in only few of the selected pairs for tunnel allocation comply with the length constraint.

We propose a heuristic, Weighted Tunnel Allocation (WTA), to better utilize the network resources than CB-STA. Instead of finding node pairs for the tunnel allocation without considering the tunnel length constraint, WTA only take node pairs that comply with the length constraint into consideration. A novel auxiliary graph model is constructed to facilitate tunnel allocation for these node pairs. The auxiliary graph is constructed by adding edges to the original topology on the node pairs whose shortest hop distance comply with the predefined length constraint. By routing the historical traffic on the auxiliary graph, preference of tunnel allocation for each node pair incident to the auxiliary link can be estimated. Finally the tunnels will be allocated according to the preference.

The remainder of this chapter is organized as follows. In Section 2, we briefly describe the node architecture used in our study, which was proposed in [HoMa01]. Section 3 gives the basic concepts on the tunnel allocation problem and the assumptions our study is based on. In Section 4, we briefly describe the CB-STA in [HoMa01] and then present our heuristic WTA. Simulation results are given in Section 5. The chapter concludes in Section 6.

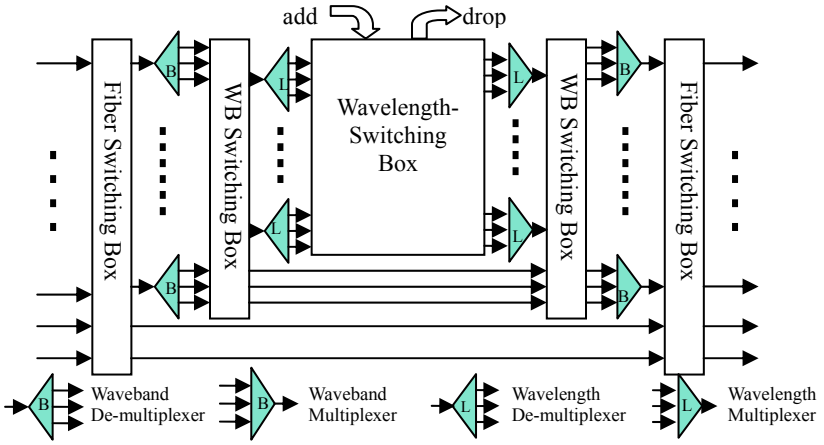

Fig. 1 Architecture of an MG-OXC.

II. Multigranularity Optical Cross Connects (MG-OXC)

The node architecture [HoMa01], shown in Fig. 1, used in our study is described as follows. A MG-OXC mainly comprises fiber-, waveband-, and wavelength-switching boxes and waveband and wavelength multiplexer/de-multiplexers. The fiber- and waveband-switching boxes on the left-hand

side serve as selectors on the input fibers and wavebands while the fiber- and waveband-switching boxes on the right-hand side serve as OXCs that switch fibers and wavebands. In a network comprising of MG-OXCs, a tunnel is a group of consecutive wavelength channels that are bundled and switched together as a single unit, which is either a fiber or waveband tunnel. All of the channels in a waveband or fiber tunnel must be switched together. A wavelength-switching port is required when a lightpath enters or exits a tunnel so that the traffic can be grouped or de-grouped. In Fig. 2, there is a tunnel between node *A* and node *C*. A lightpath from node *A* to node *C* can be established by traversing that tunnel. Note that the number of wavelength-switching ports the tunnel consumes at the two ends of the tunnel is equal to the number of the wavelengths that the tunnel carries.

The advantage of using MG-OXC is cost reduction in the switch fabric. Fig. 3 gives an example. Assume that there are ten wavelengths in a fiber and a node has two fibers coming in and going out. In Fig. 3 (a), the traditional OXC uses a 20×20 wavelength switch. However, in Fig. 3 (b), the MG-OXC uses a 10×10 wavelength switch and two 4×4 fiber switches. Although cost savings can be achieved by using MG-OXCs, it reduces the throughput and the performance of the networks. For example, in Fig. 3 (b), the traffic in the fiber can be accessed by de-multiplexing only one of the two fibers into wavelengths. The traffic in the other fiber can only bypass this node since no wavelength-switching ports can be used to de-multiplex the wavelengths in this fiber. Therefore, it needs a carefully designed tunnel allocation algorithm to achieve better tradeoff between the cost savings and performance degradation.

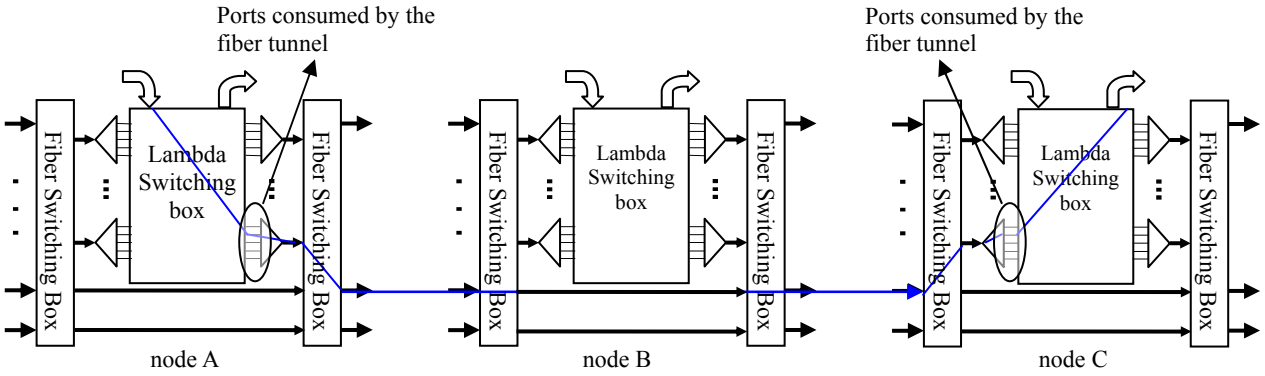

Fig. 2 MG-OXCs with two switching tiers of wavelength-switching and waveband-switching.

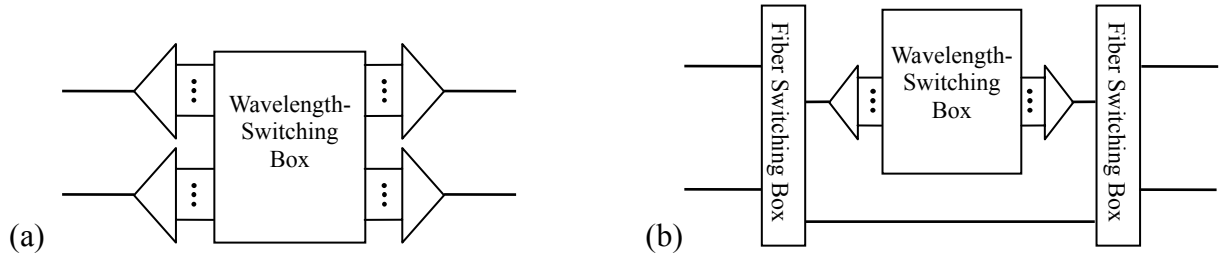

Fig. 3 (a) Traditional OXC. (b) MG-OXC.

III. Basic Assumptions and Tunnel Allocation Characteristics

This section describes the basic assumptions our study is based on. A directional link in network with MG-OXCs consists of F fibers, in which F_1, F_2, and F_3 fibers are assigned as fiber-switched, waveband-switched, and wavelength-switched fibers respectively (i.e. $F = F_1 + F_2 + F_3$). Each node is assumed to be equipped with sufficient wavelength conversion capability in the wavelength-switching layer. Therefore, a lightpath in the wavelength-switching layer can be converted into any other wavelength if necessary. The tunnels are restricted to traverse only on their shortest paths from their ingress to egress node thus increasing the efficiency of the network resource consumption.

A tunnel can be allocated between a node pair, if there is free capacity on each link along its route. Note that for the waveband tunnel, it has to use the same waveband on each link along the route. To bring up an allocated tunnel, wavelength-switching ports are further required at the two ends of the tunnel. We assume that a historical traffic matrix is known a priori and the incoming dynamic requests follow the historical traffic matrix. This information is certainly useful for us to allocate tunnels off-line before the serving lightpath requests to decrease the blocking probability and improve network throughput.

Fig. 4 illustrates ways of tunnel allocation when the tunnel length is restricted to two. Fig. 4 (a) is part of the physical network. Four fibers, A→B, B→D, D→C and C→A, are used for tunnel allocation. Fig. 4 (b) and (c) show the two possible ways of tunnel allocation. The total traffic trend should be considered when deciding which tunnel set is suitable. For example, if most traffic is between node *A* and node *D*, the tunnel set in Fig. 4 (b) is more suitable. If most traffic is between node *B* and node *C*, the tunnels are allocated as in Fig. 4 (c).

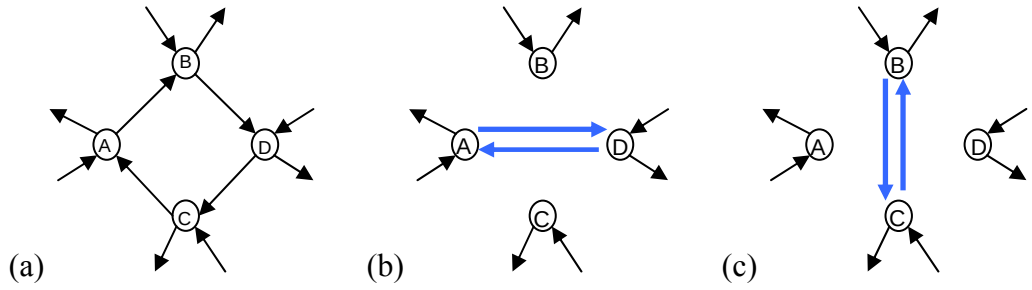

Fig. 4 (a) Physical links to allocate tunnels. (b) and (c) Two ways of tunnel allocation.

IV. Weighted Tunnel Allocation (WTA)

We first introduce previous work on tunnel allocation proposed in [HoMa01], named Capacity-Balanced Static Tunnel Allocation (CB-STA). Then we propose our heuristic Weighted

Tunnel Allocation (WTA) that aims to improve CB-STA. CB-STA allocates tunnels off-line before start serving the lightpath requests. The process comprises three stages: 1) tunnel ingress-egress (I-E) pair selection, 2) tunnel allocation and 3) makeup process. In 1), a series of I-E pairs are selected sequentially for the next stage. To select I-E pairs, CB-STA estimates the amount of traffic traveling through each node by routing the historical traffic matrix in the network. Then the nodes with maximal traffic going out and maximal traffic coming in are selected repeatedly for tunnel allocation. In 2), CB-STA tries to allocate a tunnel for each I-E pair selected in 1). Stage 3) is performed to further utilize the remaining resources to fill the fiber- and waveband-switching layer with as many tunnels as possible.

Note that tunnels allocated at stage 2) is required to follow a tunnel length constraint, which is set to the minimum integer that is larger than the average physical hop distance between each node pair in the network. This is because when the tunnel length is too small, although the short tunnels are flexible and easily utilized by most of the lightpaths, the wavelength-switching ports are used up easily since the wavelength-switching ports are required at the ingress and egress nodes of each tunnel. When the tunnel length is too large, although wavelength-switching ports can be greatly saved, the tunnels may not be suitable for the requests since most of the lightpath requests are shorter than the tunnels. We observe that the I-E pairs selected in stage 1) of CB-STA does not consider the tunnel length constraint, leading to the result that most of the tunnels are allocated at stage 3), leaving the performance of CB-STA some space to be improved.

Instead of finding node pairs for tunnel allocation without considering the tunnel length constraint, WTA only takes node pairs whose hop distance comply with the length constraint into consideration. Only those node pairs possess the potential to be allocated tunnels. WTA is based on an auxiliary graph used to rate the preference of tunnel allocation for each node pair. The process comprises four stages: a) construction of auxiliary graph, b) weight calculation for edges in the auxiliary graph, c) weighted auxiliary graph based tunnel allocation, and d) makeup process. Details are described as follows.

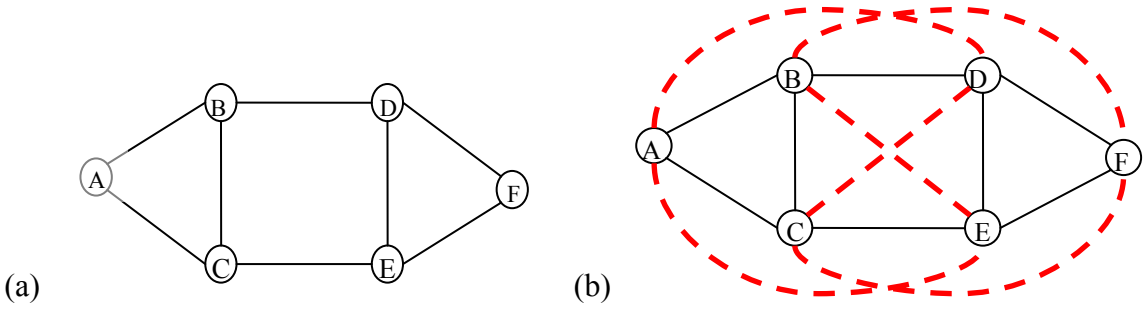

Fig. 5 An example of auxiliary graph. (a) Network topology with average hop distance 2. (b)

Corresponding auxiliary graph.

a) construction of auxiliary graph Let $G(V, E_p)$ be the original topology where V denotes the set of nodes and E_p represents the set of all physical links connecting the nodes. The auxiliary graph $G'(V, E')$ is constructed by adding auxiliary links E_l between the node pairs that have their shortest physical hop length follow the length constraint (i.e., $E' = E_p + E_l$). The auxiliary links represent the potential tunnels that could be allocated on the network. Fig. 5 gives an example of construction of auxiliary graph where Fig. 5(a) is the original topology with the average hop distance equal to two and Fig. 5(b) is the corresponding auxiliary graph.

b) weight calculation for edges in the auxiliary graph The weight of an auxiliary link is actually the predicted summation of loads on the tunnels between the nodes incident to that link. The historical traffic matrix is taken as the input traffic. We assume that the traffic for each node pair is evenly distributed on its shortest paths on the auxiliary graph. Fig. 6 gives an example of how the weights are derived. There are three shortest paths from node s to d. Traffic from s to d is assumed to be evenly distributed on the three paths. Therefore, node pair (s, d) contribute one third of its traffic on each link traversed by the three shortest paths. Weight of an auxiliary link is calculated by summing up the traffic of each node pair flowing through that link. The larger the weight of an auxiliary link, the higher chance the node pair for that link will be allocated tunnels.

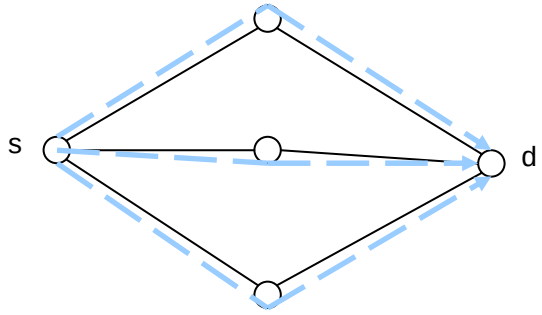

Fig. 6 An example of deriving the weight for each link in the auxiliary graph.

c) weighted auxiliary graph based tunnel allocation This stage applies a greedy approach to allocate a set of tunnels according to the weight derived in the previous stage. The auxiliary link in G' with the maximum weight is first selected, and an attempt is made to allocate a fiber tunnel for this auxiliary link. If a fiber tunnel can be successfully allocated, the weight of this auxiliary link is decreased by $\delta_F = \Psi_{\text{total}} / (U_F + U_B/B)$, where Ψ_{total} denotes the total weight of all auxiliary links, B the number of wavebands in a fiber, U_F and U_B the upper bound of the number of fiber and waveband tunnels respectively. U_F and U_B are calculated by $|E_p| \cdot F_1 / D$ and $|E_p| \cdot F_2 \cdot B / D$ respectively, where $|E_p|$ is the number of directional links on the topology and D the tunnel length

constraint. If it fails to allocate a fiber tunnel, we try to allocate a waveband tunnel for this auxiliary link. If a waveband tunnel can be successfully allocated, the weight of this auxiliary link is decreased by $\delta_B = \Psi_{\text{total}} / (U_F \cdot B + U_B)$. If both fiber and waveband tunnels fail to be allocated, the weight of this auxiliary link is set to 0. The above procedure is repeated until all of the weights of the auxiliary links in G' are equal to or less than 0.

d) makeup process This process is used to further utilize the remaining resource after stage (c). Tunnels allocated in this stage do not have to follow the length constraint.

The following summarizes the WTA.

Step1. Form the auxiliary graph by adding all possible tunnels to the physical network.
Step2. Compute weight for each possible tunnel by routing the traffic matrix on the auxiliary graph
Step3. Stop if the weight for each auxiliary link is smaller or equal to 0.
Step4. Try to allocate fiber tunnel for the auxiliary link with maximum weight. If successful, decrease the weight of this auxiliary link by δ_F and go to Step 3. Otherwise, go to Step 5.
Step5. Try to allocate waveband tunnel for this auxiliary link. Decrease the weight of this auxiliary link by δ_B. Go to Step 3.

In WTA and CB-STA, a tunnel is allocated if free link capacity on the route between the ingress and egress of the tunnel is available. An allocated tunnel needs to be further brought up to be utilized by lightpaths. When a tunnel is brought up, wavelength-switching ports are needed so that wavelengths can be group or de-group at two ends of the tunnel. The number of wavelength-switching ports consumed at each end of the tunnel so that the tunnel can be brought up is equal to the capacity (in wavelength) of that tunnel. Therefore, a Port-Constraint Weighted Tunnel Allocation (PC-WTA) is proposed with modification on WTA. In PC-WTA, after a tunnel is allocated, wavelength-switching ports at the ingress and egress nodes of the tunnel are dedicated to the tunnel. That is, a tunnel can not be allocated if any on the two ends of the tunnel has insufficient wavelength-switching ports. PC-WTA improves the performance when the wavelength-switching capability is significantly fewer than the resources in the fiber-switching and waveband-switching layers. Performance of the schemes described above is evaluated in the following section.

V. Simulation Results

The topology we use is a 16-node network show in Fig. 7. We assume that each directional link has five fibers. Each fiber contains forty wavelengths which are divided into four wavebands with wavelength 1 to 10 in the first waveband, 11 to 20 the second, …, and 31 to 40 the forth. The traffic

is uniformly distributed on all node pairs and each request is for a lightpath. The inter-arrival time between two requests is determined by the poisson distribution function with rate ρ, and the request holds the resources it traverses for a time period determined by an exponential distribution function with rate 1. We denote $(F_1)F(F_2)B(F_3)L$ the experiment with F_1 fibers for fiber-switching, F_2 fibers for waveband-switching, and F_3 fibers for wavelength-switching for each directional link.

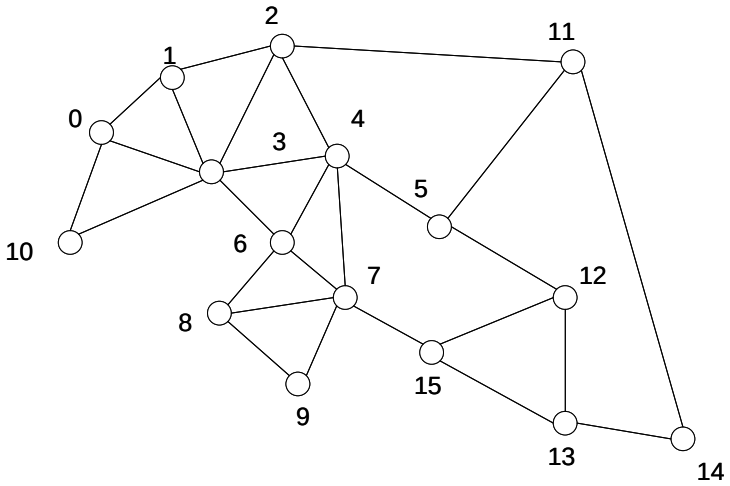

Fig. 7 The 16-node network for this simulation.

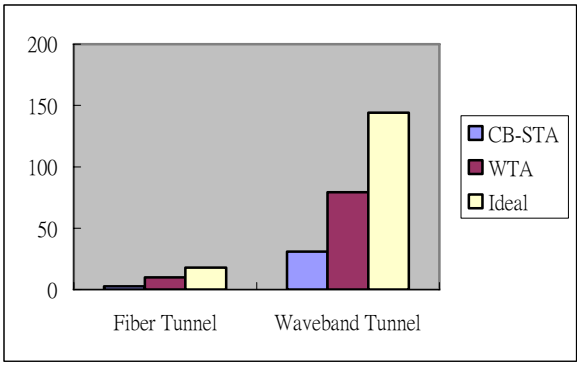

Fig. 8 Comparison of the number of allocated tunnels in WTA and CB-STA (without performing their makeup processes), and the ideal numbers under 1*F*2*B*2*L*.

Fig. 8 compares the number of allocated tunnels when CB-STA and WTA are used without performing their makeup process. The ideal number of allocated fiber tunnels and waveband tunnels are U_F and U_B, respectively. The number of allocated fiber/waveband tunnels without makeup process in CB-STA is considerably smaller than the ideal number. The reason is that most of the I-E pairs selected in CB-STA do not follow the tunnel length constraint.

Fig. 9 compares different blocking probability of the WTA and CB-STA under different load ρ. The relaxed CB-STA relaxes the length constraint D in CB-STA. More specifically, in relaxed

CB-STA, tunnels with lengths between D-1 and D+1 are permitted to be allocated. Therefore, more useful tunnels can be allocated in relaxed CB-STA than in CB-STA. The following three combinations of switching type are examined: 1F1B3L, 1F2B2L and 2F2B1L. The results show that WTA has the lowest blocking probability in all switching type combinations. The reason is that WTA allocates more tunnels that comply with length constraint while in CB-STA and relaxed CB-STA, length constraint is not carefully considered in their I-E pair selection stages.

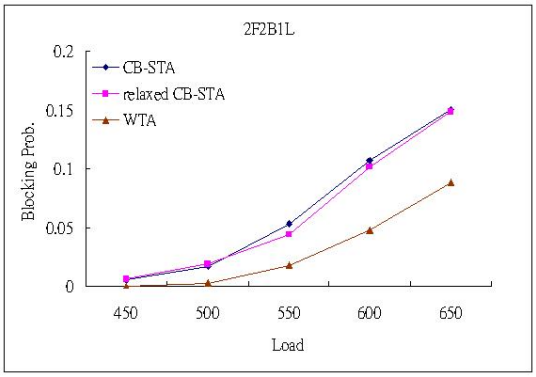

(a)

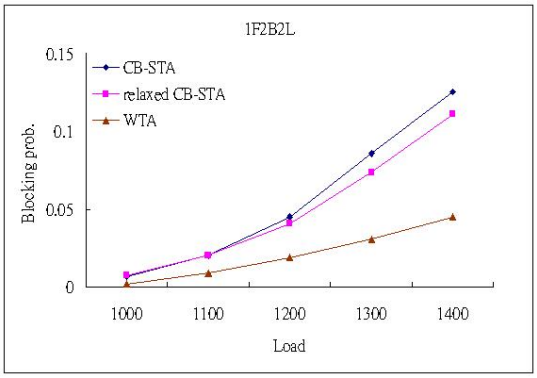

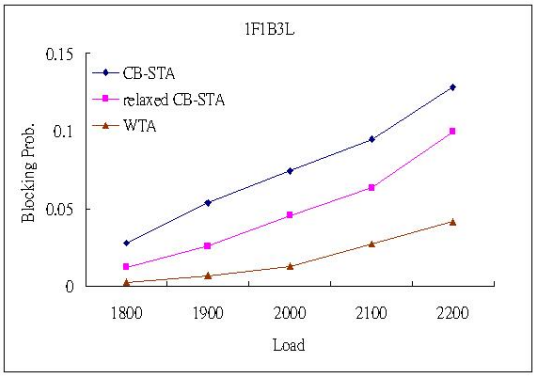

(b) (c)

Fig. 9 Comparison of blocking probability vs. load for WTA and CB-STA on the 16-node topology.

PC-WTA outperforms WTA when each node in the MG-OXC network has only limited wavelength-switching ports (in Fig. 10 (a)). That is because tunnels in PC-WTA are only allocated between nodes that have sufficient wavelength-switching ports. The link capacity and wavelength-switching ports are more efficiently utilized since most of them are consumed by the auxiliary links with higher weights. However, when there are sufficient wavelength-switching ports, performance of PC-WTA is the same as WTA (i.e., performance curves of the two algorithms in Fig.10 (b) and (c) overlaps).

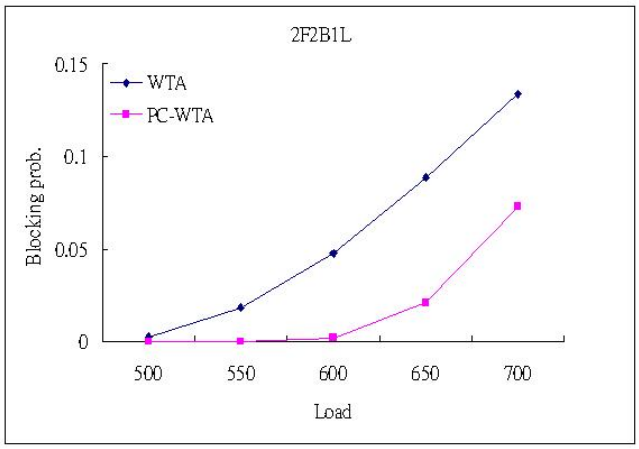

(a)

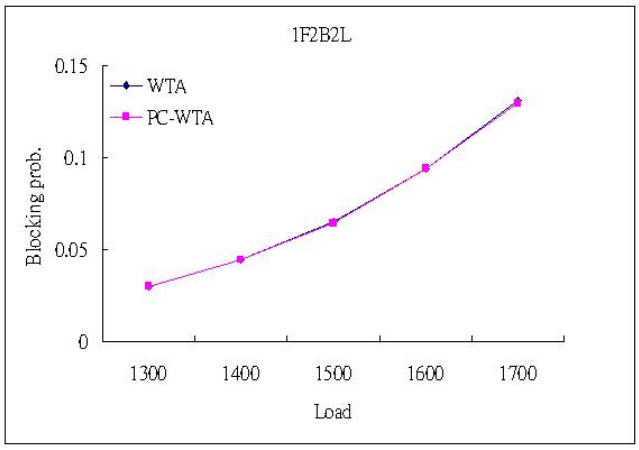

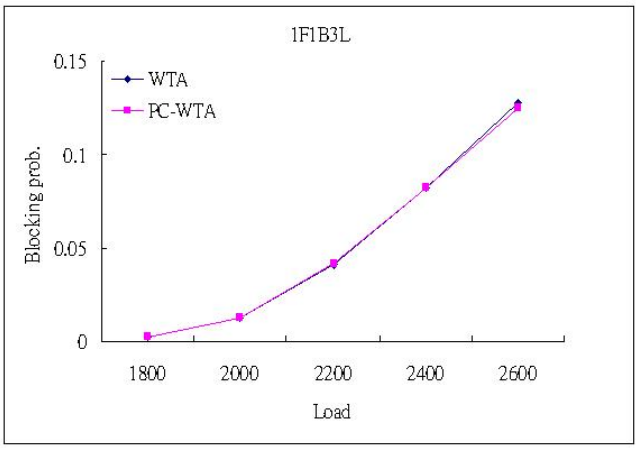

(b) (c)

Fig. 10 Comparison of blocking probability vs. load for WTA and PC-WTA on the 16-node topology.

VI. Conclusion

In this chapter, we consider the static tunnel allocation problem in the MG-OXC networks that employ a three-stage multiplexing scheme of fiber, waveband and wavelength. The previous work CB-STA does not consider the tunnel length constraint during the I-E pair selection stage, resulting in few tunnels being allocated during the tunnel allocation stage. We propose a novel auxiliary graph model for our heuristics, Weighted Tunnel Allocation (WTA) and Port-Constraint Weighted Tunnel Allocation (PC-WTA), to improve CB-STA. In WTA, tunnel allocation is only attempted for the auxiliary links, whose physical hop distances comply with the length constraint. PC-WTA furthermore, takes wavelength-switching ports into consideration while allocating tunnels. The

simulation results show that WTA outperforms CB-STA in all switching type combinations. Besides, PC-WTA has lower blocking probability than WTA when there are limited wavelength-switching ports at each node in MG-OXC networks.

Chapter 3. A New Model for Optimal Routing and Wavelength Assignment with Fixed-length Tunnel Allocation in Multigranularity Cross-connect WDM Networks

I. Introduction

Wavelength-division-multiplexing (WDM) networks have emerged as a method of providing Terabits-per-second capacity for ever-increasing bandwidth demands. Such a network is composed of optical cross-connects (OXCs) interconnected by fiber links, with each fiber supporting tens to hundreds of wavelength channels. End users in the network communicate with each other via one or several all-optical channels, i.e., lightpaths, with transmission rate ranging from one to tens of Gigabits per second.

Although increase in number of wavelength channels and fibers between node pairs may increase the available capacity, this may cause a scalability problem in maintenance and manufacturing of the optical cross-connects (OXCs). An effective way of handling this problem is to bundle a group of consecutive wavelength channels together and switch them as a single unit on a specific route to reduce the required resources of intermediate cross-connects along the route. The tunnel-like passage created by the bundled wavelength channels is defined as a waveband/fiber tunnel. Wavelengths in a tunnel must be switched together except at the two ends of the tunnel. Nodes that support such multigranularity switching, e.g. wavelength, waveband and fiber-switching, are termed hierarchical cross-connects or multigranularity optical cross-connects (MG-OXCs).

Generally, the research topics about MG-OXCs can be categorized into (a) being given the network resources and minimizing the blocking probability of the coming requests, and (b) the dimension of the network resources when given the set of traffic requests. In [Hash01], the merits of hierarchical OXC, or MG-OXC, were summarized such as small-scale modularity, reduced cross-talk, and the reducing of complexity. [NoVi01] showed that the number of ports required when grouping of consecutive lightpaths were applied to the network could be significantly reduced. In [HoMa01], a novel switching architecture, MG-OXC, was proposed to minimize the blocking probability for the dynamic requests given the limited network resources. In [LeYu01], which employs a two-stage scheme of waveband and wavelength, an integer linear programming (ILP) formulation and a heuristic are given that aim to minimize the size of optical switch matrix under the minimum link loading. However, the model suffers from the defect that only lightpaths with the same destination can be grouped in. In [CaAn01], both ILP and heuristic were given to dimension the needed ports by grouping lightpaths with any sources and any destinations. Continuing with [CaAn01], [CaAn02] further compares Single-Layer MG-OXCs and Multi-Layer MG-OXCs under

both off-line and on-line traffic. In [HoMo02], the authors try to expand the traditional OXCs for the growing traffic demand by attaching waveband- and fiber-switching boxes to the traditional OXCs. They formulate the problem into a constraint programming (CP) and give an ILP-based heuristics to solve the problem.

This chapter considers the following network design problems. In static RWA problem it is assumed that set of lightpath requests to be set-up in the network is known initially. Given the fixed amount of network resources, the objective here is to minimize the blocking probability for routing and wavelength assignment problem with fixed-length tunnel constraint. In dynamic RWA problem lightpath requests between source and destination pairs are set up on demand. Given the fixed amount of network resources and a historical traffic matrix that the dynamic requests will follow, the objective is to determine a set of tunnels off-line such that the blocking probability of the upcoming traffic requests is minimized. The heuristic Capacity-Balanced Static Tunnel Allocation (CB-STA) [HoMa01] has been proposed and it restricts that tunnels are required to follow a length constraint in order to utilize the wavelength-switching ports efficiently. CB-STA first estimates the amount of traffic traveling through each node by routing the historical traffic matrix in the network. Then the nodes with maximal traffic going out and coming in are selected repeatedly for tunnel allocation. However, since CB-STA does not consider the tunnel length constraint when picking such node pairs, only a few of the selected pairs for tunnel allocation comply with the length constraint. Therefore, a makeup process at last has to be performed to fully exploit the remaining capacity.

In our prior work [LoCh01], we proposed a novel auxiliary graph model that aptly incorporates the tunnel length constraint to facilitate solving tunnel allocation problem in MG-OXC networks. The heuristics Weighted Tunnel Allocation (WTA) and Port-Constraint Weighted Tunnel Allocation (PC-WTA) were proposed based this auxiliary graph model and were proved through simulation to show that they outperform CB-STA. In this chapter, we extend the auxiliary graph model to a layered one and based on which an ILP formulation is presented to achieve optimal solution under the tunnel length constraint. We conduct the simulation that compares the performance of CB-STA, WTA, PC-WTA, and ILP using small to medium sized network topologies, since for the large sized network topology, the ILP takes an intolerable amount of computation time.

The remainder of this chapter is organized as follows. In Section 2, we describe the MG-OXC network architecture which was proposed in [HoMa01], and the auxiliary graph model [LoCh01] for the fixed-length tunnel allocation. In Section 3, we first extend the auxiliary graph model to a layered one and then based on which we provide our ILP formulation. Section 4 shortly describes WTA and PC-WTA, which are developed based on the auxiliary graph. Simulation results are shown in Section 5. Section 6 concludes the chapter.

II. Fixed-length Tunnel Allocation

A. Network Architecture

The network is based on the node architecture [HoMa01] shown in Fig. 1. A MG-OXC mainly comprises fiber-, waveband-, and wavelength-switching boxes and waveband and wavelength multiplexer/de-multiplexers. The fiber- and waveband-switching boxes on the left-hand side serve as selectors on the input fibers and wavebands while the fiber- and waveband-switching boxes on the right-hand side serve as OXCs that switch fibers and wavebands. In MG-OXC networks, a tunnel is defined as a group of consecutive wavelength channels that are bundled and switched together as a single unit, which could be either a fiber or waveband tunnel depending on the size of the grouped wavelengths. All of the channels in a waveband or fiber tunnel must be switched together. A tunnel is said to be *allocated* if link capacity along the route of the tunnel is dedicated to that tunnel. For an allocated tunnel to be used by lightpaths, a sufficient number of wavelength-switching ports at the ingress and the egress of the tunnel have to be further dedicated to that tunnel so that lightpaths can be grouped or de-grouped at both ends. The number of wavelength-switching ports dedicated to the tunnel at the two ends of the tunnel is equal to the number of the wavelengths that the tunnel carries. We say that a tunnel is *brought up* if wavelength-switching port at the both end are dedicated to the allocated tunnel. Wavelength-switching ports at the two ends of the tunnel can be *freed* when there is no lightpath traversing it.

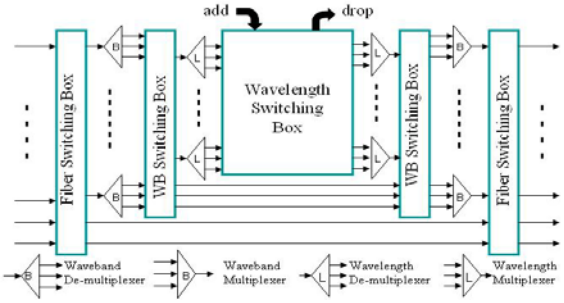

Fig 1. Architecture of an MG-OXC

In this work, we make the following assumptions. We assume that each directional link between two nodes consists of F fibers in which F_1, F_2, and F_3 fibers are assigned as fiber-, waveband-, and wavelength-switching fibers respectively (i.e. $F = F_1 + F_2 + F_3$). Accordingly, the number of ports of a node is dependent on its node degree. That is, for example, for a node i with node degree Δ_i, there are $F_3 \cdot \Delta_i \cdot |W|$ wavelength-switching ports for that node, where W is the set of wavelengths in a fiber. We also assume that each node is equipped with sufficient wavelength conversion capability in the wavelength-switching layer. Therefore, a lightpath in the wavelength-switching layer can be converted into any other wavelength if necessary. However,

waveband conversion is not assumed, and therefore waveband continuity still has to be maintained. We also assume that a tunnel can only traverse on the shortest path from its ingress node to its egress node.

B. Auxiliary Graph Model

As we mentioned in Section 1, we restricted that tunnels allocated in the MG-OXC networks should follow the tunnel length constraint to efficiently utilize the network resources. More specifically, if the value of the length constraint is set too small, the wavelength-switching ports can be used up easily. On the other hand, if it is set too large, the routing flexibility would be decreased since most of the lightpath requests are shorter than the tunnels. In our study we set the tunnel length constraint D to the minimum integer that is larger or equal to the average network hop distance. Apparently, following the tunnel length constraint, we can see that only the node pairs with their shortest hop distance equal to D could be possibly allocated tunnels. Based on this criterion, in [LoCh01] we proposed an auxiliary graph model that aptly incorporates the tunnel length constraint to facilitate solving tunnel allocation problem in MG-OXC networks. Given the network topology, the auxiliary graph is constructed by simply adding edges for those node pairs whose shortest hop distance comply with the tunnel length constraint. Fig. 2 gives an example how the auxiliary graph is constructed where Fig. 2(a) is the original network topology with average hop distance equal to 1.53, i.e., D = 2 and Fig. 2(b) is the corresponding auxiliary graph, where dashed link are inserted representing the tunnels that could be allocated between the incident nodes.

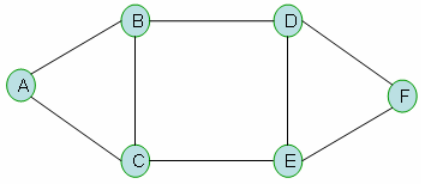

(a)

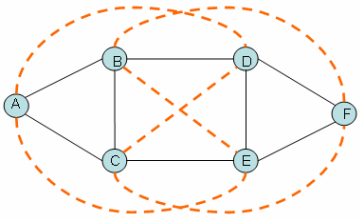

(b)

Fig.2. An example of auxiliary graph. (a) Network topology with tunnel length constraint D = 2. (b) Corresponding auxiliary graph.

In the next section, we will extend the proposed auxiliary graph model to the layered auxiliary graph model. Based on such layered graph, we propose an ILP formulation to the tunnel allocation problem.

III. Layered Auxiliary Graph and ILP Formulation

The given network can be described as follows. G (V, E) represents the network topology where V is the set of nodes and E is the set of directional links. A directional link contains $F = F_1 + F_2 + F_3$ fibers. A fiber contains $|W|$ wavelengths or $|B|$ wavebands, where W is the set of wavelengths in a fiber and B is the set of wavebands in a fiber. Our objective is to satisfy as many lightpath requests specified by a given traffic matrix Λ as possible. Our formulation can jointly determine the routing path of each established lightpath and the set of tunnels that are allocated and brought up. For the network without wavelength conversion, the wavelength assignment of each lightpath can be extended from our formulation. In the following sections, we first describe the construction of the corresponding layered auxiliary graph which our formulation is based on and then give the ILP formulation.

A. Layered Auxiliary Graph

A layered auxiliary graph is denoted by G' (V', E'). To avoid confusion, we use the terms *node* and *link* to represent a vertex and an edge, respectively in G (V, E), and we use the terms *vertex* and *edge* to represent a vertex and an edge, respectively in G' (V', E'). The construction of G' is described as follows. For each node $i \in V$, replicates it three times in G' and denote them as v_i^L, v_i^B, and v_i^F respectively, where the superscript L, B, and F indicate that they are in the wavelength-switching, waveband-switching, and fiber-switching layer, respectively. That is, $V' = V^F \cup V^B \cup V^L$, where $V^F = \{ v_i^F \mid i = 1 \sim |V| \}$, $V^B = \{ v_i^B \mid i = 1 \sim |V| \}$ and $V^L = \{ v_i^L \mid i = 1 \sim |V| \}$. We refer to waveband-switching layer and fiber switching layer together as the tunnel layers.

For each node $i \in V$, an additional edge is created to connect between each pair of the vertices v_i^L and v_i^B, and v_i^B and v_i^F in G'. These edges are called *inter-layer edges*, meaning that the lightpaths can traverse between tunnels and wavelength-switching layers. For every link (l, m) $\in E$, there are F_3 number of edges from v_l^L to v_m^L. These edges correspond to the number of

wavelength-switching fibers from node l to node m. For every node pair (i, j) in G that complies with the tunnel length constraint, there are $F_1 \cdot h_{ij}$ number of edges from v_i^F to v_j^F and $F_2 \cdot h_{ij} \cdot |B|$ number of edges from v_i^B to v_j^B, where h_{ij} is the number of shortest paths in G from node i to node j and B is the set of wavebands in a fiber. Each of these edges represents a tunnel that could possibly be traversed by the lightpaths. In the layered auxiliary graph G' (V', E'), we refer to all the additional edges in the tunnel layers as *tunnel edges*. Obviously, the final construction of the auxiliary graph is a multigraph graph. Thus, we use a three-tuple notation (v_l, v_m, p) to distinguish the different edges between vertices v_l and $v_m \in V'$. We denote edges in wavelength-switching layer, waveband-switching layer, fiber switching layer, and inter-layer edges as E^L, E^B, E^F and E^I, respectively. That is, $E' = E^L \cup E^B \cup E^F \cup E^I$.

Fig. 3 illustrates how a layered auxiliary graph is constructed assuming that $F_1 = F_2 = F_3 = 1$, $|B| = 2$, and tunnel length constraint $D = 2$. The colored edges in Fig. 4 represent the potential fiber and waveband tunnels that could be brought up in the optimization process. There are, for example, four edges from v_2^B to v_3^B since there are two shortest paths, i.e., 2-1-3 and 2-4-3, from node 2 to node 3 ($h_{23} = 2$) and two wavebands in a fiber ($|B| = 2$). The dashed edges in tunnel layers just show the physical topology and do not really exist in the graph.

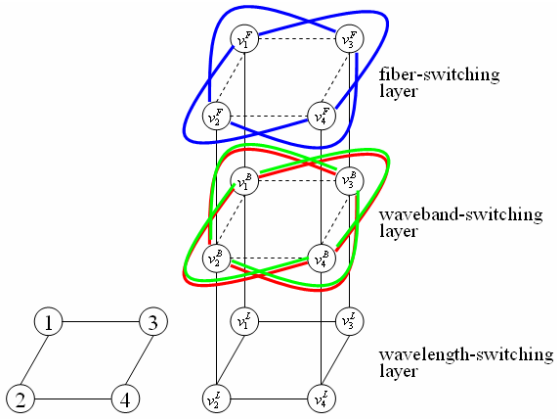

Fig. 3. Illustration of constructing a layered auxiliary graph. A network topology and the corresponding layered auxiliary graph.

B. ILP Formulation

The following notations are invariables. $R = \{(s_n, d_n) \mid n = 1 \ldots \sum_{i,j \in V} \Lambda_{ij}\ , s_n, d_n \in V\}$ represents a set of source-destination pairs requesting lightpath connections. $WS(v_i, v_j, p) = \{w \mid w \in W$ is the wavelength within the tunnel (v_i, v_j, p), $(v_i, v_j, p) \in E^F \cup E^B\}$. $PF_{(l, m)} = \{(v_i, v_j, p) \mid (v_i, v_j, p) \in E^F$ is a fiber tunnel and its corresponding physical path passes through link $(l, m)\}$. $PB_{(l, m, b)} = \{(v_i, v_j, p) \mid (v_i, v_j, p) \in E^B$ is a waveband b tunnel and its corresponding physical path passes through link $(l, m)\}$. The variables used in the formulation are defined as follows. Notably, they are all binary variables. $f(s_n, d_n)$, $n = 1 \sim |R|$, is 1 if a lightpath request (s_n, d_n), is satisfied, and 0 otherwise. For each edge $(v_i, v_j, p) \in E'$, $x^{n,w}_{v_i, v_j, p}$, $n = 1 \sim |R|$, $w \in WS(v_i, v_j, p)$, is 1 if the n-th lightpath request traverses edge (v_i, v_j, p) in wavelength w, and 0 otherwise. For each tunnel edge $(v_i, v_j, p) \in E^F \cup E^B$, $M_{v_i, v_j, p}$ is 1 if the edge is brought up, and 0 otherwise. The optimization is formulated as a 0/1 ILP shown below.

$$\text{Maximize} \quad \sum_{(s_n, d_n) \in R} f(s_n, d_n) \tag{1}$$

Subject to

$$\sum_{(v_i, v_j, p) \in E', w \in WS(v_i, v_j, p)} x^{n,w}_{v_i, v_j, p} - \sum_{(v_j, v_k, p) \in E', w \in WS(v_j, v_k, p)} x^{n,w}_{v_j, v_k, p} = \begin{cases} f(s_n, d_n)\ , \text{if } v_j = v^L_{d_n} \\ -f(s_n, d_n)\ , \text{if } v_j = v^L_{s_n} \\ 0\ \ , \text{otherwise} \end{cases} \tag{2}$$

$$, \text{for } (s_n, d_n) \in R \text{ and } v_j \in V'$$

$$\sum_{(s_n, d_n) \in R} x^{n,w}_{v_i, v_j, p} \le 1\ , \text{for} (v_i, v_j, p) \in E^L \cup E^B \cup E^F \text{ and } w \in WS(v_i, v_j, p) \tag{3}$$

$$\sum_{w \in WS(v_i, v_j, p), (s_n, d_n) \in R} x^{n,w}_{v_i, v_j, p} \ge M_{v_i, v_j, p}\ , \text{for } (v_i, v_j, p) \in E^B \cup E^F \tag{4}$$

$$|W| \cdot M_{v_i, v_j, p} \ge \sum_{w \in WS(v_i, v_j, p), (s_n, d_n) \in R} x^{n,w}_{v_i, v_j, p}\ , \text{for } (v_i, v_j, p) \in E^B \cup E^F \tag{5}$$

$$\sum_{(v_i,v_j,p)\in PF_{(l,m)}} M_{v_i,v_j,p} \le F_1 \quad \text{, for } (l,m) \in E \tag{6}$$

$$\sum_{(v_i,v_j,p)\in PB_{(l,m,b)}} M_{v_i,v_j,p} \le F_2 \quad \text{, for } (l,m) \in E \text{ and } b \in B \tag{7}$$

$$\begin{aligned} &|W| \times \sum_{(v_j^F,v_k^F,p)\in E^F} M_{v_j^F,v_k^F,p} + \frac{|W|}{|B|} \times \sum_{(v_j^B,v_k^B,p)\in E^B} M_{v_j^B,v_k^B,p} \\ &+ \sum_{(v_j^L,v_k^L,p)\in E^L,(s_n,d_n)\in R,w\in W} x_{v_j^L,v_k^L,p}^{n,w} \le F_3 \cdot |W| \cdot \Delta_j \quad \text{, for node } j \in V \end{aligned} \tag{8}$$

$$\begin{aligned} &|W| \times \sum_{(v_i^F,v_j^F,p)\in E^F} M_{v_i^F,v_j^F,p} + \frac{|W|}{|B|} \times \sum_{(v_i^B,v_j^B,p)\in E^B} M_{v_i^B,v_j^B,p} \\ &+ \sum_{(v_i^L,v_j^L,p)\in E^L,(s_n,d_n)\in R,w\in W} x_{v_i^L,v_j^L,p}^{n,w} \le F_3 \cdot |W| \cdot \Delta_j \text{ , for node } j \in V \end{aligned} \tag{9}$$

The objective function (1) aims to satisfy as many lightpath requests as possible. Equation (2) stipulates the flow conservation constraint for a specific lightpath request. Equation (3) shows that each wavelength in each edge $(v_i, v_j, p) \in E^F \cup E^B \cup E^L$ can be used just once. Equation (4) says that a tunnel won't be brought up if there's no lightpath traversing through that tunnel, while Equation (5) says that a tunnel must be brought up if any lightpath traverses it. Equation (6) constrains that the number of fiber tunnels traversing a link cannot exceed the number of fiber-switching fibers on that link. Similarly, equation (7) constrains that the number of waveband tunnels of a waveband b traversing a link cannot exceed the number of waveband-switching fibers on that link for all $b \in B$. Equation (8) and (9) describe the wavelength-switching port constraint on the egress side (output port) and ingress side (input port) of an OXC node, respectively, where Δ_j is the node degree of node j in G. The first term on the left-hand side of equation (8) summarizes a node's wavelength-switching output ports consumed by the fiber tunnels that start from that node. Similarly, the second term summarizes those consumed by the waveband tunnels. The third term summarized those consumed by the lightpath bypassing or starting from that node. The summation of these three terms cannot exceed the number of wavelength-switching output ports that the node has. In the same way, equation (9) indicates that the summation of a node's wavelength-switching input ports consumed by the fiber tunnels and waveband tunnels that ending at that node, and the lightpath bypassing or ending at that node should not exceed the number of wavelength-switching input ports. Fig. 4 illustrates the wavelength-switching output ports consumed by the ingress of a fiber (Fig. 4(a)) and a waveband tunnel (Fig. 4(b)).

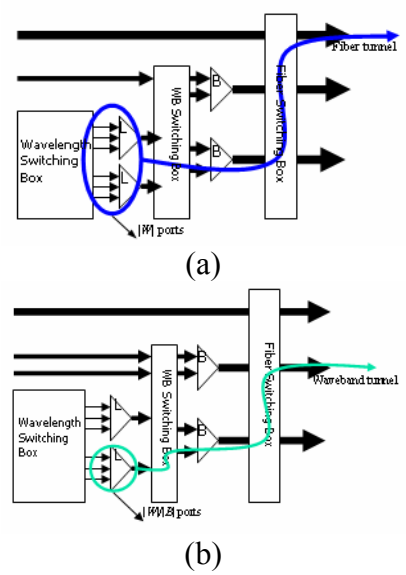

Fig.4. Illustration for equation (8). (a) Ingress of a fiber tunnel consumes $|W|$ wavelength-switching ports. (b) Ingress of a waveband tunnel consumes $|W|/|B|$ wavelength-switching ports.

IV. Auxiliary Graph Based Heuristic Algorithms

In this section, we shortly describe the heuristics WAT and PC-WTA [LoCh01], which are based on our auxiliary graph model. In WTA, an auxiliary graph is first constructed (see Fig. 2). After that, to estimate the load that the edges in the auxiliary carry, we temporarily route all the traffic demands on the auxiliary graph. Note that the expected load on the edges connecting the node pairs that comply with the tunnel length constraint now represent the expected load that would flow on the tunnels constructed for them. Then we enter the tunnel allocation stage that repeatedly picks the edge with the maximum expected load and try to allocate a tunnel for it. The success or failure of allocating a tunnel is determined by whether there is sufficient link capacity along any of its shortest paths. The heuristic is ended by a makeup process that tries to utilize any remaining resource that could be allocated tunnels. However, in this chapter, we will not perform any makeup process in all heuristics and ILP in order to have fair comparison.

PC-WTA is basically WTA with a slight difference when allocating tunnels. In PC-WTA, a tunnel is successfully allocated for a node pair only if the link capacity along any of its shortest paths and wavelength-switching ports at the ingress and egress nodes of the tunnel are available. This modification is to prevent allocating too many non-critical tunnels such that it would consume wavelength-switching ports efficiently. As expected, the simulation results following will show that PC-WTA performs better than WTA when the wavelength-switching capability is significantly fewer than the resources in the fiber-switching and waveband-switching layers.

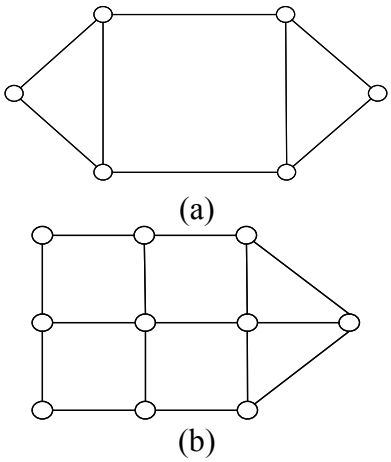

Fig. 5. Network topologies adopted in our simulation. (a) 6-node network topology. (b) 10-node network topology.

V. Simulation Results

The set of tunnel determined by our heuristics can be applied to both static traffic and dynamic traffic. For the static traffic, where all the traffic demands are known in advance, the performance differs as the order in which the requests are routed changes. After we adopt WTA as the major heuristic that determines the set of tunnels, we use the following schemes as the routing sequence to compare the simulation results with the ILP solution. The ILP is solved by LINDO optimizer [web01].

- *Random* : the sequence to route the requests is randomly chosen.
- *Shortest Path First* : the request with the shortest hop distance on the network topology from the source to the destination is chosen first to be routed.
- *Longest Path First* : the request with the longest hop distance on the network topology from the source to the destination is chosen first to be routed.

We use the 6-node network topology shown in Fig. 5(a) with $|W| = 4$ and $|B| = 2$. A set of 50 requests are randomly generated among different node pairs. (F_1)F(F_2)B(F_3)L stands for the experiment with F_1 fibers for fiber-switching, F_2 fibers for waveband-switching, and F_3 fibers for wavelength-switching in each directional link on the network topology. The results are shown in Table I. The numbers in the table are the blocking probability of the total requests. We observe that among the three schemes of routing sequence, Shortest Path First performs best while Longest Path First has the worst performance. Also, the case of 1F1B1L performs better than that of 2F1L due to the better switching flexibility.

TABLE I
Comparison Of Different Traffic Routing Sequence Under WTA With The ILP Solutions.

	ILP	WTA		
		Random	Shortest	Longest
1F1B1L	0.12	0.272	0.176	0.348
2F1L	0.12	0.280	0.178	0.360

For the dynamic traffic, we compare the performance of ILP, CB-STA, WTA, and PC-WTA using the small and medium sized network topologies shown in Fig. 5(a) and (b). We assume that $|W| = 4$ and $|B| = 2$. The historical traffic matrix Λ is randomly generated. This traffic matrix is used as the input traffic for the ILP process and the heuristics. Note that the ILP formulation assumes that the traffic is static. Therefore, we will discard the routing information of each request in ILP solution and only take the set of tunnels allocated. The obtained set of tunnels is used to accommodate the dynamic requests. The dynamic traffic is generated with request arrival rate following a Poisson distribution with rate ρ. Source and destination of each request is determined by the probability $\Lambda_{i,j} / \sum \Lambda_{i,j}$. The request holding time is determined by an exponential distribution function with rate 1.

Fig. 6 shows the simulation results. Each datum is derived by running 50000 requests. It can be observed that WTA and PC-WTA outperform CB-STA in both networks. In the 6-node network, PC-WTA outperforms WTA (Fig. 6(a) and (b)) and in the 10-node network, PC-WTA and WTA even perform almost the same as the ILP solution (Fig. 6(c) and (d)). Comparing Fig. 6(a) and (b), we also observe that 1F1B1L performs better than 2F1L, and for Fig. 6(c) and (d), though it is not obvious, 1B1L is slightly better than 1F1L. This is legitimate since the more fibers are dedicated to the fine-grained switching type, the more flexible the routing of the requests is.

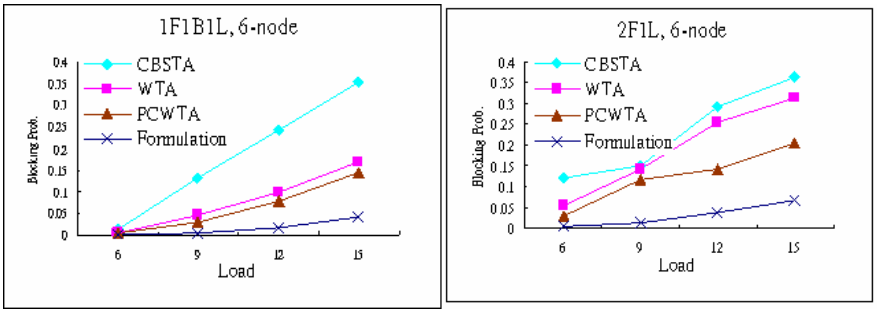

(a) (b)

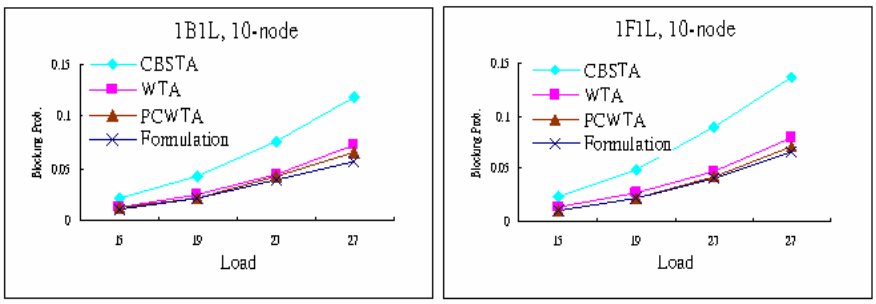

(c) (d)

Fig.6. Comparison results of CB-STA, WTA , PC-WTA and ILP under different switching type combination and network topologies. (a) 1F1B1L , 6-node network. (b) 2F1L, 6-node network. (c) 1F1L, 10-node network. (d) 1B1L, 10-node network.

VI. Conclusion

In this chapter, we consider the problem of RWA with tunnel allocation in the MG-OXC networks. We propose an ILP formulation that gives the optimal solution for the static traffic under the tunnel length constraint. We extend the auxiliary graph model from our previous work to the layered auxiliary graph model to facilitate our ILP formulation. This allows us to consider the RWA and fix-length tunnel allocation sub-problems simultaneously in order to exploit optimal solution. We conduct the simulation experiments to compare the performance between different heuristics and the ILP solution. We first determine a set of fix-length tunnels using WTA, which are based on the auxiliary graph model [LoCh01]. Then we adapt one of the routing sequence schemes to route the static traffic over the tunnels. The simulation results show that WTA with the Shortest Path First scheme reaches nearest to the optimal solution. For the dynamic traffic, the results show that WTA and PC-WTA outperform CB-STA significantly. In the 10-node network topology, the performance of WTA and PC-WTA is even compatible with optimal solution. We also observed that PC-WTA outperforms WTA when the number of wavelength-switching ports is small. In MG-OXC networks wavelength-switching ports are critical resources and PC-WTA utilizes the wavelength-switching ports more efficiently.

Chapter 4. Design of Tunnel-based Protection Schemes in Multigranularity Optical Cross-connect Networks

I. Introduction

Wavelength-division multiplexing (WDM) optical networks are widely accepted as the solution for supporting the growing demands of bandwidth. Recently, hierarchical optical cross-connects, or multi-granularity Optical Cross-connects (MG-OXCs) [HoMa01][NoVi01][LoCh01] are even gaining more and more research attention due to their attractiveness in saving the network cost. The principal idea of MG-OXC networks is to bundle a group of consecutive wavelength channels together and switch them as a single unit on their common sub-path so that the required ports of intermediate cross-connects along the route can be reduced. The bundled channels form the so-called waveband or fiber tunnels in which lightpaths can not be wavelength-switched except at the ends of the tunnels. In this chapter, we aim to provide an efficient fault-recovery protection scheme for the lightpaths in the MG-OXC networks.

Basically, protection schemes can be classified into path protection, link protection, and the compromise of the previous two, segment protection. The protection schemes can be further categorized into shared protection and dedicated protection. In dedicated protection, different backup paths do not share any link in the same wavelength plane. To share the backup resources, the constraint is that two backup paths cannot share wavelengths on the links if their corresponding working paths have common links. Obviously, shared protection utilizes bandwidth more efficiently than dedicated protection. Nevertheless, it is at the expense of recovery time because in shared protection, cross-connects can not be pre-configured to save the reconfiguration time [XuXi01].

The protection problem in MG-OXC networks has only been considered in [VaJu01]. The authors propose a graph-based heuristic that tries to minimize the total number of switch ports in the network, given a set of static connection requests. Our study differs from [VaJu01] because we assume that the network resource is already given and the node architecture is the multi-layer MG-OXC proposed in [HoMa01] instead of the single-layer MG-OXC. The problem is described as follows. Given the network resources and a historical traffic matrix that the future requests will follow, provide a shared protection scheme that minimizes the blocking probability of future requests under the constraint so that for each request, both working path and backup path must be found to guarantee 100% survivability.

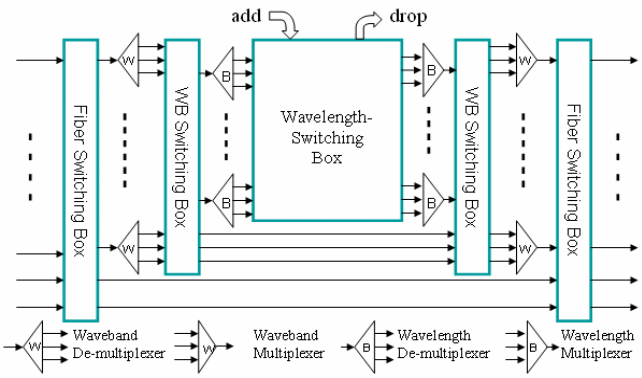

Fig. 1. Architecture of the MG-OXC

II. Protection Schemes in MG-OXC Networks

The MG-OXC architecture [HoMa01] is shown in Fig. 1. In the MG-OXC network, a directional link consists of $F = F_1 + F_2 + F_3$ fibers, where F_1, F_2 and F_3 fibers are assigned as fiber-, waveband-, and wavelength-switched fibers, respectively. In a waveband- or fiber-switched fiber, all the wavelengths in a waveband or a fiber have to be switched together. Depending on the size of the grouped wavelengths, the tunnel-like passage formed by the grouped wavelengths, which is switched as a single unit, is termed as a waveband tunnel or a fiber tunnel.

Intuitively, the protection problem in MG-OXC networks can be divided into two phases: 1) off-line tunnel allocation and 2) finding link-disjoint lightpaths for each incoming request. A straightforward solution is to allocate tunnels off-line without protection consideration and then find two link-disjoint lightpaths from source to destination for each incoming request. We call this scheme Tunnel Based Path Protection (TPP). Although TPP provides a protection solution for the networks with MG-OXC, the lack of protection consideration in the first phase complicates the finding of link-disjoint lightpaths since two tunnels sharing any common link can not be utilized by a working path and its backup path. Therefore, we propose another scheme called Tunnel Based Segment Protection (TSP). In TSP, a working tunnel is always allocated followed by the allocation of a backup tunnel. Consequently, MG-OXC network protection problem can be formed into one kind of segment protection problem.

A. Tunnel Based Path Protection (TPP)

It should be noted that while allocating tunnels, we only take tunnels that comply with length constraint into account [HoMa01]. The length constraint forces all tunnels to have equal length to simplify tunnel allocation. If the value of the length constraint is set too small, the wavelength-switching ports can be used up easily. On the other hand, if it is set too large, the routing

flexibility would be decreased since most of the lightpath requests are shorter than the tunnels. In our study we set the tunnel length constraint to the average hop distance.

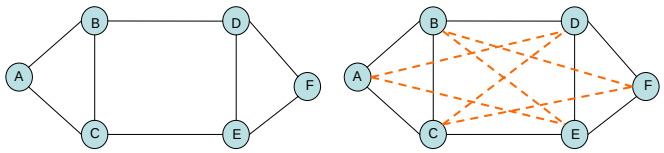

(a) (b)

Fig. 2. (a) The original network topology with average hop distance equal to two. (b) The corresponding auxiliary graph.

We first transform the physical network topology into an auxiliary graph by adding edges, which we term as potential tunnel edges, between nodes whose shortest hop length follows the length constraint. Fig. 2 demonstrates the construction of the auxiliary graph. After the auxiliary graph is constructed, the historical traffic matrix is temporarily routed on the auxiliary graph with the assumption that the load between each node pair will be equally distributed on all its shortest paths. After finish the routing of all traffics, the total load, or weight, on each potential tunnel edge by this time is just the estimated load between the nodes incident to that edge, and the larger the value the higher priority it gets to be allocated as a tunnel. We then pick up the potential edge with the largest weight, allocate a tunnel for it and decrease its weight for a fixed amount of value. This process is repeated until all the weight of the potential edges are less than or equal to zero. Details of this process can be found in [LoCh01].

After the tunnels are allocated on the network, we can start to serve the incoming requests. For each request, both working path and protection path should be found or the request should be blocked. For example, in Fig. 3, two link-disjoint paths are found for request (S, D).

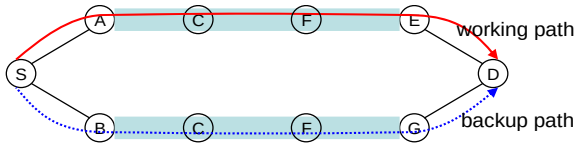

Fig. 3. An example of TPP.

B. Tunnel Based Segment Protection (TSP)

TSP operates similarly to TPP except that whenever allocating a tunnel for a node pair, a backup tunnel should also be allocated. Consequently, a working path for a request can be segmented according to the switching types along its route. Since the segments in the tunnel layer are already protected by their backup tunnels, only those segments in the wavelength-switching

layer need to be further protected. Fig. 4 gives a layered view of this concept. A working path from node A to node F (A-B-D-F), shown as the red solid line, is divided into A-B-D and D-E, where segment A-B-D is protected in the tunnel-switching layer by backup tunnel A-C-E-D and segment D-E is protected in the wavelength-switching layer by backup lightpath D-E-F.

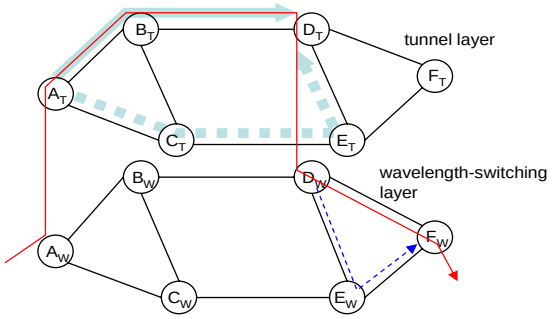

Fig. 4. A layered view for the concept of TSP.

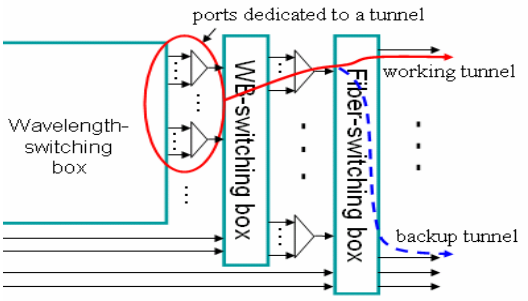

Fig. 5. MG-OXC only reconfigures the fiber-switching box to switch the traffic in working tunnel to protection tunnel

We deduce that TSP provides better performance than TPP (in terms of blocking probability) for two reasons. The first comes from the intrinsic superiority of resource sharing efficiency in segment protection than in path protection. Second, a backup tunnel in TSP can use the same wavelength-switching ports, which is the critical resource in MG-OXC networks, with its working tunnel. Once a link failure occurs and results in breakdown of a working tunnel, we only have to reconfigure the fiber- or waveband-switching boxes on the backup path while leaving the wavelength-switching ports at the two ends of the tunnel unchanged. Fig. 5 shows the port sharing on the ingress side of a working fiber tunnel and its backup tunnel. In contrast to TSP, there is no sharing of wavelength-switching ports between tunnels in TPP, thus a lightpath request may require more wavelength-switching ports.

III. Simulation Results

We evaluate the performance of TPP and TSP via simulation using a 16-node topology. We assume that each directional link has five fibers. Each fiber contains forty wavelengths which are evenly divided into four wavebands. Each node is assumed to have enough wavelength conversion capability, but there is no waveband conversion. (*F1*)F(*F2*)B(*F3*)L stands for the experiment with *F*1 fibers for fiber-switching, *F*2 fibers for waveband-switching, and *F*3 fibers for wavelength-switching in each directional link. The traffic is assumed to be uniformly distributed. Each request is randomly generated among all node pairs and once satisfied, it remains on the network until simulation ends.

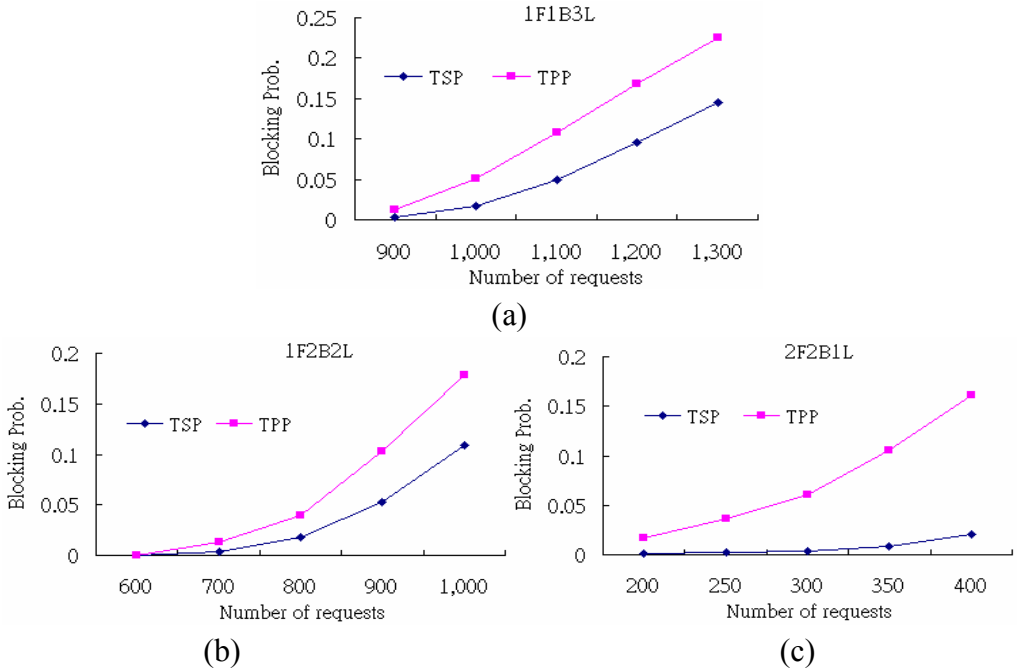

Fig. 6. Comparison of TSP and TPP under different combination of switching types. (a)1F1B3L. (b)1F2B2L. (c)2F2B1L.

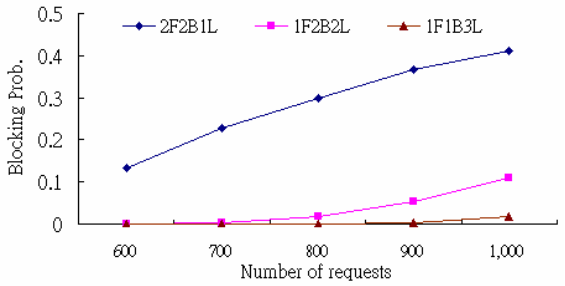

Fig. 7. Traffic load vs. blocking probability in different switching combinations in TSP.

Fig. 6 shows the simulation results. Blocking probability increases as *F1* and *F2* increase. The results show that TSP outperforms TPP in all switching type combinations. We also observe that the fewer fibers dedicated to the wavelength-switching layer, thus less wavelength switching ports, the larger the difference of blocking probability between TSP and TPP. For example, in 1F1B3L, TSP is 43% better than TPP in terms of blocking probability when there are 1200 requests. In 1F2B2L, TSP is 48% better than TPP when there are 900 requests. Furthermore, in 2F2B1L, TSP is 91% better than TPP when there are 350 requests. This indicates that wavelength-switching ports are critical resource in the MG-OXC networks. Fig. 7 demonstrates this point more clearly. It shows that the less of the traffic is blocked with the more wavelength-switching ports. The wavelength-switching ports influence the performance of the networks significantly, thus it makes sense to derive an algorithm that can save ports. TSP can save ports by letting a pair of working and protection tunnel use the same ports, thus it will have better performance.

IV. Conclusion

In this chapter, we investigate the protection schemes for the single link failure in the MG-OXC networks. Path protection based scheme TPP provide a straightforward resolution. However, the absence of taking protection requirement into consideration when allocating tunnels propels us to provide another scheme, TSP, to improve the performance of TPP. In TSP, a backup tunnel is always allocated with a working tunnel. Hence, the working path of a lightpath request can be naturally segmented according to the switching types along its route, with each segment protected in its corresponding layer. In addition to the intrinsic superiority of resource sharing in segment protection than in path protection, TSP also utilizes less wavelength-switching ports for a lightpath request. Simulations are conducted to compare the performance of TPP and TSP. The results show that TSP outperforms TPP in terms of blocking probability, due to the better sharing efficiency of TSP in link capacity and wavelength-switching ports.

Chapter 5. Virtual Topology Reconfiguration in Hierarchical Cross-connect WDM Networks

I. Introduction

With the rapid increase of IP traffic, there is no doubt that in the near future data communications will be based on optical networking. Wavelength-division-multiplexed (WDM) networks are considered to be one of the most promising future transport infrastructures to meet the ever-increasing bandwidth demand. Such networks consist of optical cross-connects (OXCs) interconnected by fiber links, with each fiber supporting a number of wavelength channels. End users in the networks communicate with each other via all-optical channels, i.e., lightpaths, where each of which may span a number of fiber links to provide a "circuit-switched" interconnection between two nodes.

A virtual topology is defined to be the set of such lightpaths in a network. Design of virtual topology is the problem of optimizing the use of network resources for the given traffic demands among all node pairs. In real networks, the traffic rates between node pairs fluctuate over time. A virtual topology optimized for a specific traffic pattern may not work as appropriate to a different one. Therefore, reconfiguration of virtual topology is needed to adjust to the new traffic pattern. A literature survey of virtual topology reconfiguration can be found in [LeMe01]. Authors in [RaRa01] and [BaMu01] show the virtual topology reconfiguration using the linear programming formulation. The formulations ensure that the new configuration is not too different from the original virtual topology so that number of reconfiguration steps can be minimized. In [TaZh01]and [TaZh02], the authors propose several reconfiguration algorithms that attempt shift from one virtual topology to another while keeping the disruption of the network minimum. They focus on the process of transforming the virtual topology from the original to the new one but not on finding the optimal virtual topology for the new given network traffic pattern.

With current technologies, the huge fiber bandwidth can be divided into 100 or more wavelengths. However, as the number of wavelength channel increases, the number of ports needed at OXCs also increases, making the size of OXCs too large to implement and maintain. Recently, several types of multigranularity optical cross-connects (MG-OXCs) [HoMa01][HaSh01][NoVi01] have been proposed to handle such scalability problem. The principle of the MG-OXC network is to bundle a group of consecutive wavelength channels together and switch them as a single unit on a specific route so that the number of ports needed by the intermediate nodes along the route can be reduced.

Although MG-OXCs are gaining more and more research attentions, literature has not yet been

seen on the virtual topology reconfiguration problem in such networks. In this chapter, we study the virtual topology reconfiguration problem in the networks using MG-OXC architecture (shown in Fig. 1) as proposed in [HoMa01]. In such a network, a directional link consists of $F = F_1 + F_2 + F_3$ fibers, where F_1, F_2 and F_3 fibers are assigned as fiber-, waveband- and wavelength-switched fibers, respectively. In a waveband- or fiber-switched fiber, all the wavelengths in a waveband or a fiber have to be switched together. The tunnel-like passage formed by the grouped wavelengths that are transmitted as a single unit is termed as a waveband tunnel or a fiber tunnel, depending on the size of the grouped wavelengths. For a lightpath to utilize a tunnel, wavelength-switching ports are required both at the ingress and the egress of the tunnel

In this chapter, we assume that the future traffic pattern can be accurately predicted, i.e., known a priori and the basic traffic unit is a lightpath. Therefore, instead of reconfiguring the lightpaths in the tradition OXC networks for the sub-wavelength granularity traffic, here we concern about reconfiguring tunnels in the MG-OXC networks for the lightpaths. We consider the following problem. Given V_1, T_1 and T_2, where V_1 is a set of tunnels allocated based on current traffic pattern T_1, and T_2 is the future traffic pattern, the objective is to reconfigure V_1 with little changes as possible while minimizing the blocking probability for T_2. We propose the heuristic called Preference Based Reconfiguration Algorithm (PBRA) to solve the problem. An auxiliary graph is used to rate the preference of each existent and nonexistent tunnels by routing the future traffic (T_2) on it. According to the obtained preference, small number of tunnels will be updated to reconfigure the original virtual topology for the new traffic pattern.

The remainder of this chapter is organized as follows. Section II presents details of PBRA. Simulation results are given in Section III. The chapter concludes in Section IV.

II. Preference Based Reconfiguration Algorithm

Although short tunnels are easily utilized by most of the lightpaths, the wavelength-switching ports can be used up easily since the wavelength-switching ports are required at the ingress and egress nodes of each tunnel. Long tunnels, on the other hand, though save wavelength-switching ports, may not be suitable for the requests since most of the lightpath requests are shorter than the tunnels. Therefore, we restrict that the tunnels follow the tunnel length constraint, i.e., the length of each tunnel should be the same, which is set to the minimum integer that is larger than the average distance of paths between each s-d pair in the network [HoMa01][LoCh01].

PBRA is based on an auxiliary graph to rate for each node pair the preference of having tunnels established between them. We then determine the addition, deletion or keeping of the tunnels based on the derived preference value. Since the length constraint can be derived from the given physical

topology, we can determine the set of node pairs that is qualified to be allocated tunnels easily. That is, only the node pairs whose shortest path distance equal to the length constraint could be allocated tunnels. This is reflected in the construction the auxiliary graph. The whole process comprises four stages: (a) construction of auxiliary graph, (b) cost assignment for edges in the auxiliary graph, (c) load estimation of existent and nonexistent tunnels, and (d) tunnel selection. Details are described as follows.

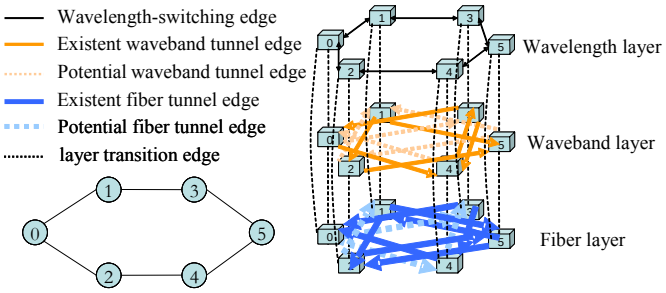

Fig. 2. Illustration of the construction of auxiliary graph. (a) The physical topology (b) The corresponding auxiliary graph

(a) Construction of auxiliary graph

Let $G_p(V_p, E_p)$ be the physical topology where V_p denotes the set of nodes and E_p is the set of all physical links connecting the nodes. The auxiliary graph $G_a(V_a, E_a)$ mainly comprises three layers, which are wavelength waveband and fiber layers and is obtained as follows. Each node $i \in V_p$ is replicated into wavelength, waveband and fiber layer. These nodes are denoted as V_i^W, V_i^B and $V_i^F \in V_a$. If edge $e \in E_p$ connects node i to node j, $i, j \in V_p$, then node V_i^W is connected to V_j^W by a directed edge, termed wavelength-switching edge. For each node pair *i-j* with existent waveband (fiber) tunnel in V_1, the node V_i^B (V_i^F) is connected to V_j^B (V_j^F) by a directed edge, termed existent waveband (fiber) tunnel edge. For each node pair *i-j* with its shortest physical hop length follow the length constraint and has not yet been allocated waveband (fiber) tunnel, there is also an edge connecting from V_i^B to V_j^B (V_i^F to V_j^F), termed potential waveband (fiber) edge. For each node $i \in V_p$, there are bidirectional edges between V_i^W, V_i^B, and V_i^F, termed layer transition edges. Fig. 2 gives an example of construction of the auxiliary graph. Fig. 2(a) is the physical topology with its average hop distance equal to two. The corresponding auxiliary graph may be the one shown in Fig. 2(b).

(b) Cost assignment for edges in the auxiliary graph

Costs of the edges are assigned as in Table I.

TABLE I
COST FOR EDGES IN G_a

Existent waveband (fiber) tunnel edge	D (Length constraint)
Potential waveband (fiber) tunnel edge	D'+ scale
Wavelength-switching edge	>>D
Layer transition edges	0

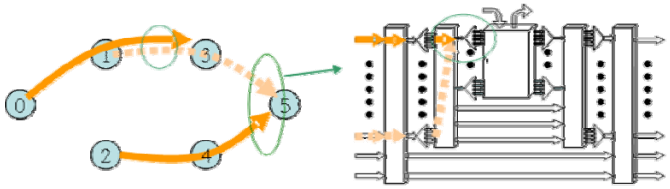

Fig. 3. Illustration of calculating *CL*. (a) Conflictions happen at physical links and at end nodes. (b) A detailed drawing of the confliction at the end nodes.

Since we hope to reconfigure V_1 with little changes, the existent tunnel edges have the smallest cost D which is the tunnel length constraint. D' is used to adjust the degree of preference on the existent tunnels where $D' \geq D$ and $D' \in \mathbf{Z}$. The higher D' we select the less preference the existent tunnels will be used. For each potential waveband (fiber) edge, a scale is associated with it. The scale represents the degree of difficulty to construct a tunnel for the node pair associated with that edge. The more existent tunnels must be deleted to construct a tunnel for a potential tunnel edge, the larger the scale is for that potential tunnel edge. Scale for potential tunnel edge i is defined to be $(CL_i - CL_{min}) / (CL_{max} - CL_{min})$, where CL_i is the number of existent tunnels that may hinder the construction of the tunnel for the node pair associated with edge i, $CL_{max} = \max_{j \in \text{potential tunnel edges}} CL_j$ and $CL_{min} = \min_{j \in \text{potential tunnel edges}} CL_j$. Figure 5 illustrates the calculation of *CL* for the potential tunnel edge. Note that the conflictions between the existent and nonexistent tunnels may happen at physical links or the end nodes of the tunnels (They contend for the wavelength switching ports). In Fig. 3(a), the thick and dash lines represent the actual physical paths of existent and nonexistent tunnels, respectively. The nonexistent tunnel (1, 5) conflicts with the existent tunnel (0, 3) at the physical link (1, 3) and with the existent tunnel (2, 5) at the end node 5 (Fig. 3b). Thus, the CL for the potential tunnel edge (1, 5) is 2.

(c) Load estimation of existent and nonexistent tunnels

After completion of stage (b), we can then route T_2 on the auxiliary graph to estimate the load on each edge of the auxiliary graph. We assume that the load between each node pair will be equally

distributed on all its shortest paths. For example, for the network shown in Fig. 2, assume that the future traffic between node 0 and node 5 is 10 and five shortest paths are found as shown in Fig. 4(a). Then each of the five paths will be distributed 2 units of the load. After T_2 is routed on the auxiliary graph, for each node pair, the summation of the load of the existent/potential waveband/fiber edges for that pair will be recorded in a matrix W. Fig. 4(b) shows the matrix W as a result of Fig. 4(a) where $W_{0,4} = 2$, $W_{1,5} = 2 + 2 = 4$ and $W_{2,5} = 2 + 2 = 4$.

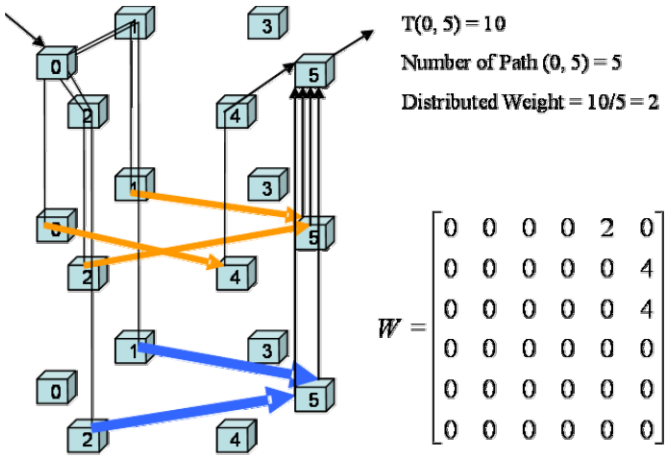

Fig. 4. Computation of W. (a) Five shortest paths from node 0 to node 5. (b) The corresponding W.

(d) Tunnels selection

W is used to determine the set of tunnels. The process repeatedly examine the node pair with the maximum weight to see whether there are existent tunnels for the node pair, otherwise, it tries to construct a new tunnel for the node pair. If there are already existent tunnels allocated between the selected pair, keep one of them in the virtual topology. Otherwise, construct a tunnel between the selected pair and if necessary, delete the existent tunnels that hinder the construction. Note that whether keeping or constructing a tunnel, the fiber tunnel is considered first. If a fiber tunnel is kept, or constructed successfully, weight of the corresponding node pair is decreased by $\delta_F = \Sigma W_{i,j}/(L \cdot F_T/D)$, where $W_{i,j}$ is the weight of the node pair (i, j), L the number of directional links in the physical topology, $F_T = F_1 + F_2$ the number of fibers dedicated to tunnel allocation in each directional link and D the length constraint. Similarly, for the waveband tunnel, the weight is decreased by $\Sigma W_{i,j}/(L \cdot B \cdot F_T/D)$, where B is the number of wavebands in a fiber. If both fiber and waveband tunnels fail to be constructed, the weight is set to 0. The whole algorithm of PBRA is summarized as follows.

Preference Based Reconfiguration Algorithm:
Input:
V_1 : Current virtual topology

T_2 : Future traffic pattern

Output:

V_2 : New virtual topology for T_2

Algorithm:

Step 1: Construct G_a.

Step 2: Define the cost for each edge in G_a and compute the weight matrix W by routing the lightpath requests of T_2 on G_a.

Step 3: Let (i, j) be the node pair with maximal weight. Stop if $W_{i,j}$ is smaller or equal to 0.

Step 4: If there are existent fiber tunnels for (i, j), keep one of them, decrease the weight of the node pair by δ_F, and go to Step 3. Otherwise, go to Step 5.

Step 5: If there are existent waveband tunnels for (i, j), keep one of them, decrease $W_{i,j}$ by δ_B, and go to Step 3. Otherwise, go to Step 6.

Step 6: Try to construct a fiber tunnel for (i, j). If successful, decrease $W_{i,j}$ by δ_F, and go to Step 3. Otherwise, go to Step 7.

Step 7: Try to construct a waveband tunnel for (i, j). If successful, decrease $W_{i,j}$ by δ_B, and go to Step 3. Otherwise, go to Step 8.

Step 8: Set $W_{i,j}$ to 0, go to Step 3.

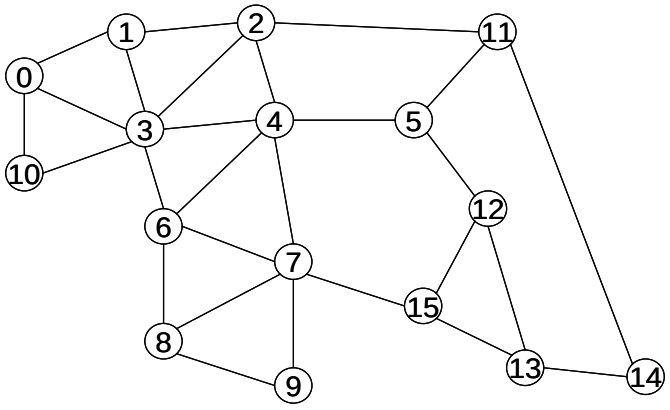

Fig. 5. Physical topology of our simulation environment

III. Simulation Results

Simulation experiments were conducted on the 16-node network shown in Fig. 5. The notation (*F1*)F(*F2*)B(*F3*)L represents the experiment with F1 fibers for fiber switching, F2 fibers for waveband switching and F3 fibers for wavelength switching on each link. We assume that a fiber contains 40 wavelengths and can be divided into four fixed wavebands, with λ_1~λ_{10} being waveband one, λ_{11}~λ_{20} waveband two…, and λ_{31}~λ_{40} waveband four. In the simulation, waveband conversion is not allowed while wavelength conversion within the bands is assumed. Two types of traffic patterns are used for the transition between old and new ones. 1) Ring traffic: the load for each node pair $(i, (i+1) \bmod 16)$, $i = 0, \ldots, 15$ is in average 10 times larger then others. 2) Uniform traffic: All traffic requests are randomly generated between each node pair.

Although not shown in the result, it is worth noting that when the new and old traffic pattern are similar, reconfiguration is unnecessary since the original virtual topology is already suitable for the new traffic pattern. Fig. 6 and Fig. 7 shows the simulation results of total number of lightpath request vs. blocking probability and percentage of unchanged tunnels under 2F1B2L and 2F2B1L. The curve "only consider T_2" means that the new virtual topology is designed without considering the original using the heuristic presented in [LoCh01] and serve as the best case for the comparison. "T_2 route on V_1" means that we directly route the new traffic on the V_1 without changing the original topology and serve as the worst case for the comparison. It can be observed that the improvement space between the two curves is rather limited. The parameter D' is tuned to observe the tradeoff.

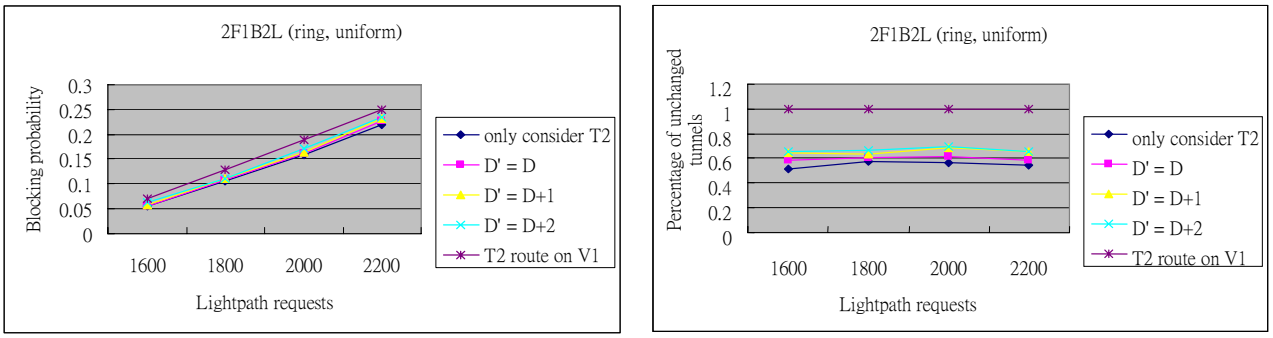

(a)

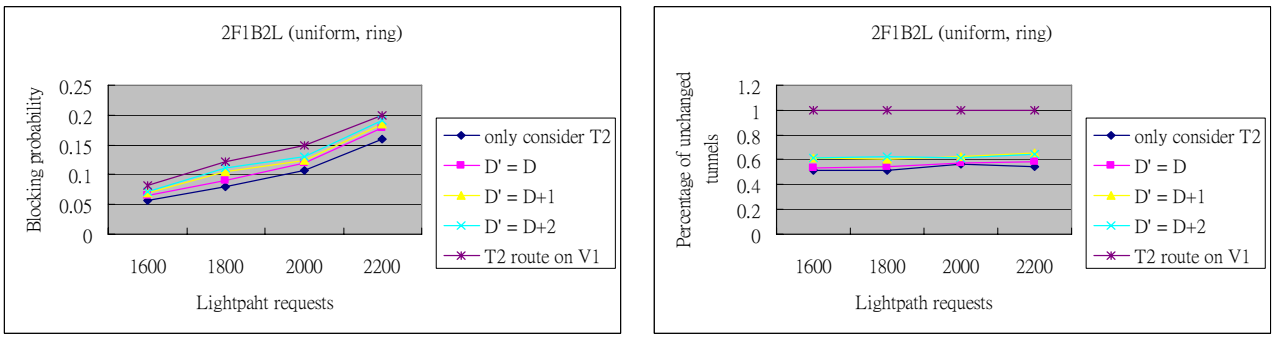

(b)

Fig. 6. Comparison of number of lightpath vs. blocking probability and percentage of unchanged tunnels (2F1B2L). (a) traffic pattern changed from ring to uniform (b) traffic pattern changed from uniform to ring

When D' gets higher, the percentage of unchanged tunnels and the blocking probability also raises. This is because higher D' means higher difficulty to construct a nonexistent tunnel, therefore resulting in more unchanged tunnels. The more unchanged tunnels then lead to the higher blocking probability. It shows that PBRA can be performed to reserve more original tunnels at the cost of little increase in the blocking probability. For example, in Fig. 6(a), while an 23% increase in the number of the unchanged tunnel under a traffic load of 2000 lightpath requests, the blocking probability increases only 0.013.

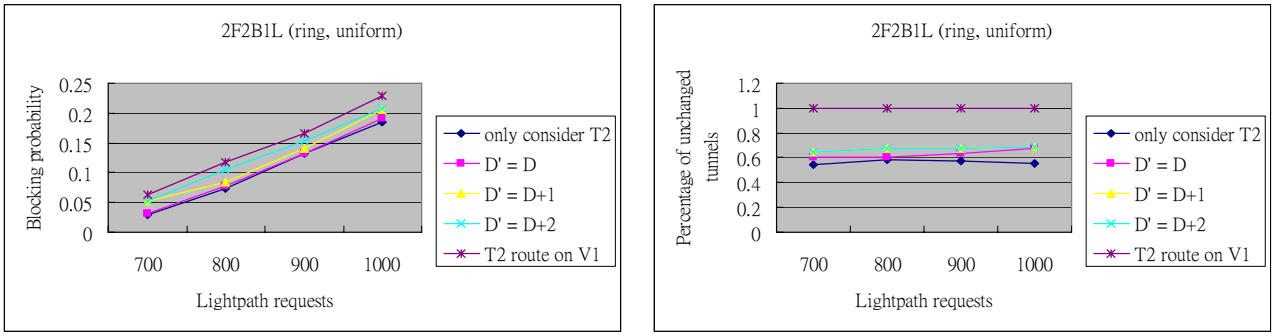

(a)

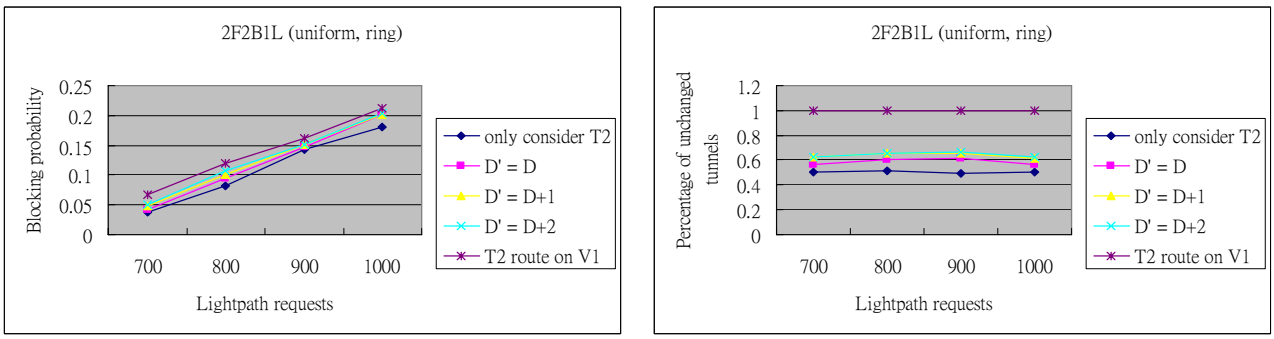

(b)

Fig. 7. Comparison of number of lightpath vs. blocking probability and percentage of unchanged tunnels (2F2B1L). (a) traffic pattern changed from ring to uniform (b) traffic pattern changed from uniform to ring

IV. Conclusion

In this chapter, we proposed a heuristic PBRA to solve the virtual topology reconfiguration in MG-OXC networks. We restricted that the tunnels should follow the length constraint and an auxiliary graph is constructed to determine the preference of having tunnels established for those potential node pairs. We show that the improvement space of performing reconfiguration in MG-OXC networks is limited since there is not much difference in blocking probability between reconfiguration if not performed and when performed without considering the original virtual topology. Nonetheless PBRA can still be performed to reserve more original tunnels at the cost of little increase in the blocking probability.

Chapter 6. Conclusion and Self-evaluation

The growth in demand changes so rapidly that it is difficult to keep up with the changes. The use of dense Wavelength Division Multiplexing technology has significantly increased the available bandwidth in backbone networks. We endeavor to capture a substantial subset of the key problems in MG-OXC networks and propose solutions to these problems. Our study results have been positively accepted in several international conferences [LoCh01][LoCh02][YeCh01][KuCh01][LiCh01] and the achievement has bring about accomplishment of four master theses[Lo01][Chen01][Yeh01][Lin01]. By executing this project, we expect to bring the most advanced research in the world to Taiwan, and potentially will become the performance benchmark for the design of next generation GMPLS networks.

References

[BaMu01] D. Banerjee and B. Mukherjee, “Wavelength-routed optical network: linear formulation, resource budgeting tradeoffs, and a reconfiguration study,” IEEE/ACM Transactions on Networking, vol. 8, no. 5, Oct., 2000, pp. 598-607.

[Berger01] L. Berger, Ed., “Generalized Multi-Protocol Label Switching (GMPLS) Signaling Functional Description ,” RFC3471, Jan 2003.

[CaAn01] X. Cao, V. Anand, Y. Xiong and C. Qiao, “Performance Evaluation of Wavelength Band Switching in Multi-fiber All-Optical Networks,” *in Proc. IEEE Infocom*, Vol. 3, Mar. 2003, pp. 2251-2261.

[CaAn02] X. Cao, V. Anand and C. Qiao, “Multi-Layer versus Single-Layer Optical Cross-connect Architectures for Waveband Switching”, *IEEE Infocom'04,* 2004.

[Chen01] Ying-Yu Chen, “Performance Evaluation of Multigranularity Switching in Hierarchical Cross-Connect WDM Networks”, Master’s thesis, 2004

[KuCh01] S. Kuo, Chien Chen, and Ying-Yu Chen, “A New Model for Optimal Fixed-length Tunnel Allocation in Multigranularity Cross-connect WDM Networks”, *IEEE Milcom*, Oct. 17-20, 2005.

[LeMe01] E. Leonardi, M. Mellia, and M. Ajmone Marsan, “Algorithms for the logical topology design in WDM all-optical networks,” Optical Networks Mag., Jan., 2000, pp. 35-46.

[LeYu01] M. Lee, J. Yu, Y. Kim, C.-H. Kang, and J. Park, “Design of hierarchical crossconnect WDM networks employing a two-stage multiplexing scheme of waveband and wavelength,” *IEEE Journal on Selected Areas in Communications*, Vol. 20, Jan. 2002, pp. 166-171.

[LiCh01] C. Lin, C. Chen, "On the design of optical buffer for optical input-queued switches with quality of service guarantees," *SPIE APOC*, Nov. 7-11, 2004.

[Lin01] Chun-Yuan Lin, “On the Design of Optical Buffer for Optical Input-Queued Switches with Quality of Service Guarantees”, Master’s thesis, 2005

[LoCh01] T. Lo, C. Chen and Y. Chen, "An effect scheme for fixed-length tunnel allocation in hierarchical WDM networks," APOC 2004, November 7~11.

[LoCh02] Tse Yu Lo, Chien Chen, and Ying Yu Chen, “Design of Tunnel-based Protection Schemes in Multigranularity Optical Cross-connect Networks”, *IEEE Broadnet*, Oct. 3-8, 2005.

[Lo01] Tse-Yu Lo, “Tunnel Allocation and Protection in Hierarchical Cross-connect WDM Networks”, Master’s thesis, 2004

[HaSh01] K. Harada, K. Shimizu, T. Kudou, and T. Ozeki, “Hierarchical optical path cross-connect systems for large scale WDM networks,” in *Proc. Optical Fiber Communications (OFC’99)*, Vol. 2, Feb. 1999, pp. 356-358.

[HoMa01] P. –H. Ho and H. Mouftah, “Routing and Wavelength Assignment with Multigranularity Traffic in Optical Networks”, *IEEE Journal of Lightwave Technology,* Vol. 20, No. 8, Aug. 2002, pp. 1992-1303.

[HoMo02] P.-H. Ho, M. T. Mouftah, and J. Wu, “A Scalable Design of Multigranularity Optical Cross-Connects for the Next-Generation Optical Internet,” *IEEE Journal on Selected Areas in Communications*, Vol. 21, No. 8, Sept. 2003, pp. 1133-1142.

[NoVi01] L. Noirie, M. Vigoureus, and E. Dotaro, “Impact of intermediate traffic grouping on the dimensioning of multi-granularity optical networks,” in *Proc. Optical Fiber Communications (OFC’01)*, Vol. 2, March 2001, pp. TuG3.1-TuG3.3.

[RaRa01] B. Ramamurthy and A. Ramakrishnan, “Virtual topology reconfiguration of wavelength-routed optical WDM networks,” IEEE GLOBECOM ’00, vol. 2, Dec. 2000, pp. 1269-1275.

[XuXi01] D. Xu, Y. Xiong, C. Qiao, “Novel algorithms for shared segment protection,” *IEEE JSAC*., vol. 21, 1320-1331, Oct. 2003.

[TaZh01] H. Takagi, Y. Zhang, and X. Jia, “Virtual topology reconfiguration for wide-area WDM networks,” IEEE International Conference on Communications, vol. 1, Jul., 2002, pp. 835-839.

[TaZh02] H. Takagi, Y. Zhang, and X. Jia, “Reconfiguration heuristics for logical topologies in wide-area WDM networks,” IEEE GLOBECOM '02, vol. 3, Nov., 2002, pp. 2701-2705.

[VaJu01] S. Varma and J. P. Jue, "Protection in Multi-Granular Waveband Networks," *IEEE Globecom* 2004, Dallas, TX, November 2004.

[web01] http://www.lindo.com/

[Yeh01] Hsiao-Yun Yeh, “Virtual Topology Reconfiguration in Hierarchical Cross-connect WDM Networks”, Master’s thesis, 2004.

[YeCh01] Hsiao-Yun Yeh, Chien Chen, and Ying-Yu Chen,“Virtual Topology Reconfiguration in Multigranularity Optical Cross-Connect WDM Networks”, *IEEE HPSR*, May 12-14, 2005.